

Supporting Information

Ultrathin Cerium Phenylphosphonate Nanosheets for Photocatalytic Cycloaddition of Carbon Dioxide to Epoxides

Soumalya Banerjee,^a Soumita Sarkar,^a Sk Afsar Ali,^a Sunny Sarkar,^a Anjumun Rasool,^b Manzoor Ahmad Dar,^b Sasanka Dalapati^c and Astam K. Patra^{a*}

^aDepartment of Chemistry, University of Kalyani, Kalyani, West Bengal 741235, India

^bDepartment of Chemistry, Islamic University of Science and Technology, Awantipora, Jammu and Kashmir 192122, India

^cDepartment of Materials Science, Central University of Tamil Nadu, Thiruvavur, Tamil Nadu 610005, India

*Corresponding author email E-mail: astamchem18@klyuniv.ac.in, [Orcid.org/0000-0001-6071-8653](https://orcid.org/0000-0001-6071-8653).

Description	Page
Chemicals	S4
Characterization Techniques	S4
Computational methods	S5
Light on-off experiment	S6
Recyclability test	S6
The Chemical and Mechanical Stability	S6-S7
Fig. S1 a) N ₂ adsorption-desorption isotherm of cerium phenylphosphonate (CPP) NSs and b) corresponding pore size distribution (PSD) curve obtained by the NLDFIT model.	S8
Fig. S2 Stability of catalyst in presence of O ₂ a) FT IR spectra and c) powder XRD pattern. Stability of catalyst under air exposure b) FT IR spectra and d) powder XRD pattern.	S8
Fig. S3 Stability of catalyst in water a) FT IR spectra and b) powder XRD pattern.	S9
Fig. S4 Mechanical stability (under sonication treatment) a) FT IR spectra, b) powder XRD pattern and c) FESEM images.	S9
Fig. S5 XPS survey profile of cerium phenylphosphonate NSs.	S10
Table S1: Summary of elemental Analysis of CPP NSs by EDX and XPS	S10
Fig. S6 Photoluminescence (PL) spectrum of cerium phenylphosphonate (CPP) NSs.	S11
Table S2: Photoelectrochemical characterization data was obtained from the Nyquist fitted plot (Fig. 5i).	S11

Fig. S7 ^1H NMR (400 MHz, CDCl_3) spectra of crude product of CO_2 cycloaddition reaction with styrene oxide after 3h reaction (Fig. 6c) over CPP NSs.	S12
Fig. S8 ^1H NMR (400 MHz, CDCl_3) spectra of crude product of CO_2 cycloaddition reaction with styrene oxide after 6h reaction (Fig. 6c) over CPP NSs.	S13
Fig. S9 ^1H NMR (400 MHz, CDCl_3) spectra of crude product of CO_2 cycloaddition reaction with styrene oxide after 12h reaction (Fig. 6c) over CPP NSs.	S13
Fig. S10 ^1H NMR (400 MHz, CDCl_3) spectra of crude product of CO_2 cycloaddition reaction with styrene oxide after 12h reaction without CPP NSs (Table 2, entry 2).	S14
Fig. S11 ^1H NMR (400 MHz, CDCl_3) spectra of crude product of CO_2 cycloaddition reaction with styrene oxide after 12h reaction over CPP NSs without light (Table 2, entry 3).	S14
Figure S12. light-on/light-off experiment for CO_2 cycloaddition reaction with styrene oxide over CPP NSs.	S15
Table S3: Standard reaction was carried out in different temperature.	S15
Fig. S13 ^1H NMR (400 MHz, CDCl_3) spectra of crude product of CO_2 cycloaddition reaction with styrene oxide after 12h reaction over CPP NSs at 50°C in dark (Table S3, entry 3).	S16
Fig. S14 ^1H NMR (400 MHz, CDCl_3) spectra of crude product of CO_2 cycloaddition reaction with styrene oxide after 12h reaction over CPP NSs at 75°C in dark (Table S3, entry 4).	S16
Fig. S15 ^1H NMR (400 MHz, CDCl_3) spectra of crude product of CO_2 cycloaddition reaction with styrene oxide after 12h reaction over CPP NSs without solvent (Table 2, entry 14).	S17
Table S4: Standard reaction was carried out in presence of different amount of TBAB.	S17
Fig. S16 ^1H NMR (400 MHz, CDCl_3) spectra of crude product of CO_2 cycloaddition reaction with styrene oxide after 12h reaction over CPP NSs with 0.2 mmol TBAB (Table S4, entry 2).	S18
Fig. S17 ^1H NMR (400 MHz, CDCl_3) spectra of crude product of CO_2 cycloaddition reaction with styrene oxide after 12h reaction over CPP NSs with 0.1 mmol TBAB (Table S4, entry 3).	S18
Table S5: Standard reaction was carried out in presence of different scavengers.	S19
Fig. S18 ^1H NMR (400 MHz, CDCl_3) spectra of crude product. The standard reaction was carried out in presence of AgNO_3 (Table S5, entry 2).	S19
Fig. S19 ^1H NMR (400 MHz, CDCl_3) spectra of crude product. The standard reaction was carried out in presence of Na_2EDTA (Table S5, entry 3).	S20
Fig. S20 ^1H NMR (400 MHz, CDCl_3) spectra of crude product. The standard reaction was carried out in presence of DMPO (Table S5, entry 4).	S20
Fig. S21 Schematic diagram of a) styrene oxide radical and b) CO_2 radical intermediates trapped by DMPO.	S21
Fig. S22 DFT optimized structure of a) styrene oxide and b) CO_2 adsorbed crystal respectively.	S21
Fig. S23 a) Recyclability of CPP NSs in the standard reactions condition. b)	S22

SEM image, c) FT IR and d) powder XRD pattern of reused catalyst.	
¹ H and ¹³ C NMR data (Table 3)	S23-S28
Table S6: Comparison of the reaction yield of allylglycidyl ether over different catalysts.	S29
Table S7: Comparison of the reaction yield of benzyl glycidyl ether over different catalysts.	S29
Table S8: Comparison of the reaction yield of epichlorohydrin over different catalysts.	S30
Table S9: Comparison of the reaction yield of phenyl glycidyl ether over different catalysts.	S31
Table S10: Comparison of the reaction yield of styrene oxide over different catalysts.	S32-S33
References	S33

Chemicals

Ceric nitrate hexahydrate (>99.0%, Spectrochem), Phenylphosphonic acid (>98.0%, TCI), Sodium hydroxide (>97.0%, Merck) and deionised water were used for materials synthesis. Styrene oxide (>97.0%, Merck), Benzyl glycidyl ether (99.0%, Merck), Phenyl glycidyl ether (>99.0%, TCI), Allyl glycidyl ether (>99.0%, TCI), Epichlorohydrin (99.0%, TCI), Butylene oxide (>99.0%, TCI), Propylene oxide (>99.0%, TCI), Tetrabutylammonium bromide (TBAB, >98.0%, Himedia), Poly ethylene glycol (PEG 600, Merck), Acetonitrile (>99.5%, Merck), DMF (>99.0%, Merck), Ethylene glycol (99.0%, Merck), Acetone (>99.0%, Finar Limited), Ethyl acetate (>99.5%, Finar Limited), Ethanol (99.9%, CSS reagent), AgNO₃ (>99.0%, Sigma Aldrich), Ethylenedinitrilotetraacetic acid, disodium salt dihydrate (>99.0%, Merck) and 5,5-dimethyl-1-pyrroline N-oxide (DMPO, 97%, BLD pharma) were used in catalytic activity test. Perfluorinated resin solution containing Nafion (Sigma Aldrich) was used in electrochemical analysis. All the chemicals were used as purchased; no further purification was done.

Characterization Techniques

The cerium phenylphosphonate nanosheets were investigated by different characterization technique. Powder X-ray diffraction patterns of the samples were recorded on a Bruker D-8 Advance diffractometer operated at 40 kV voltage and 40 mA current using Cu K α ($\lambda = 0.15406$ nm) radiation. The recorded Powder X-ray diffraction patterns were analyzed by MATCH software, Version 3.x, CRYSTAL IMPACT, Kreuzherrenstr, 102, 53227 Bonn, Germany to identify the phase of the synthesized materials. Nitrogen sorption isotherms were obtained at 77 K using an ASAP 2000 surface area analyzer (Micromeritics Instrument). Prior to the measurement, the samples were degassed at 423 K for 3 h. Fourier transform infrared (FT-IR) spectra were recorded on a Perkin Elmer-L120-000A spectrophotometer. SEM images were recorded in a JEOL JEM 6700 Field emission scanning electron microscope (FE SEM) for conducting morphology analysis. TEM images were recorded in a JEOL 2010 TEM operated at 200 kV. The EDX spectrum and corresponding elemental composition of the CPP nanosheets, is obtained from the Dark-field STEM image using JEOL 2010 TEM instrument. X-ray photoelectron spectroscopy (XPS) was performed on a Thermo Scientific (Model No ESCALAB 250Xi) X-ray Photoelectron Spectrometer operated at 15 kV and 20 mA with a monochromatic Al K α X-ray source. UV-Visible spectra were recorded out using UV-VIS spectrophotometer (Model Shimadzu-UV 2401 PC). The EPR measurements were carried out using continuous wave spectrometers operating at X-band

frequency (9–10 GHz) (BRUKER BIOSPIN, Germany, Model–EMXmicro A200–9.5/12/S/W). The electrochemical experiments were conducted using a computer-controlled electrochemical workstation (BioLogic 150e) within a standard three-electrode system. ^1H and ^{13}C NMR experiments were carried out on a Bruker Ultrashield 400 MHz NMR spectrometer.

Computational methods

Spin-polarized density functional theory (DFT) calculations were carried out using the generalized gradient approximation (GGA) in the form of Perdew–Burke–Ernzerhof (PBE) exchange-correlation functional¹ with Vienna Ab initio Simulation Package (VASP).^{2, 3} The projector augmented wave (PAW) method⁴ was used to describe the core-valence electron interactions. Considering the role of weak interactions, DFT-D3 semiempirical scheme was applied to take care of the dispersion effects between the adsorbate and the catalyst.⁵ The convergence threshold for energy was set to 10^{-5} eV and the geometries were optimised by relaxing the positions of the atoms until the forces acting on each atom is less than 0.02 eV/Å. Throughout the calculations, the kinetic energy cutoff of electronic wave function was set to 520 eV, which is sufficiently large for the systems considered here. A Γ -centered Monkhorst–Pack K-point grid of $3 \times 3 \times 1$ was used to sample the Brillouin zone for geometry optimisations, while a higher $6 \times 5 \times 1$ grid was used for electronic structure analysis. The vacuum space was set to be 20 Å in the z-direction to avoid interlayer interactions. Grid-based Bader charge analysis⁶ was used to carry the charge transfer analysis. Software packages such as VESTA⁷ and VASPKIT⁸ were used for processing the obtained calculation results.

The adsorption energy (E_{ads}) of styrene oxide adsorbate on the crystal was computed by using the below equation:

$$E_{\text{ads}} = E_{\text{sty-oxide@crystal}} - E_{\text{crystal}} - E_{\text{sty-oxide}}$$

Where $E_{\text{sty-oxide@crystal}}$ is the total energy of the styrene oxide adsorbed on the crystal species, E_{crystal} and $E_{\text{sty-oxide}}$ are the energies of crystal and the free styrene oxide molecule respectively.

The Heyd–Scuseria–Ernzerhof (HSE06) hybrid functional⁹ is used to obtain more accurate band gaps for the crystal species.

Light on-off experiment

The model experiment was conducted under specific conditions where the light source was alternately turned on and off for a period of two hours. A sample of crude from the reaction medium was collected, and the progress of the reaction was monitored.

Recyclability test

The reusability of the CPP nanosheets was examined for the above-mentioned cycloaddition reaction between CO₂ and epoxide. For the experiment, 3 mmol of epoxy styrene, 0.3 mmol of TBAB and 25 mg of cerium phenylphosphonate catalyst was taken. The reaction proceeded in PEG under UV irradiation for 12 hours. Upon completion, the catalyst was isolated by centrifugation and subjected to rigorous purification by repeated washing with ethanol and water. Finally, the catalyst was reactivated by drying at 100 °C for 3 hours before reuse. The activated catalyst underwent recyclability studies, being reused for five consecutive reaction cycles.

The Chemical and Mechanical Stability

The chemical stability of the CPP material was evaluated in the presence of O₂, air and water.

CPP stability in O₂: In this study, 50 mg of catalyst was dispersed in 25 mL of water inside a round-bottom flask, and O₂ was introduced using an attached balloon. The suspension was left under continuous O₂ exposure for three days, in room temperature. The catalyst was then recovered, dried, and analyzed by FT IR and powder XRD. The results are shown in Figure S2 in the supporting information file.

CPP stability in Air: In this experiment, 50 mg of the catalyst was placed in an oven at 55 °C for seven days to assess its stability under prolonged thermal and atmospheric exposure. This sample was also examined by FT IR and powder XRD analysis. The results are shown in Figure S2 in the supporting information file.

CPP stability in water: To test the stability of CPP material in presence of water, 50 mg of catalyst was dispersed in 25 mL of water inside a sealed round-bottom flask and left for three days, in room temperature. The catalyst was then recovered, dried, and analyzed by FT IR and powder XRD. The results are shown in Figure S3 in the supporting information file.

Mechanical Stability: Further to probe the mechanical robustness of CPP, we dispersed 50 mg of the catalyst in water, subjected it to vigorous overtaking, and sonicated the suspension for 2 hour. The recovered and dried catalyst was subsequently characterized again by FT IR, SEM, and XRD. No observable changes in functional groups, morphology, or crystallographic features were detected. These results collectively support the mechanical and structural stability of the layered catalyst under rigorous conditions. The results are show in Figure S4 in the supporting information file.

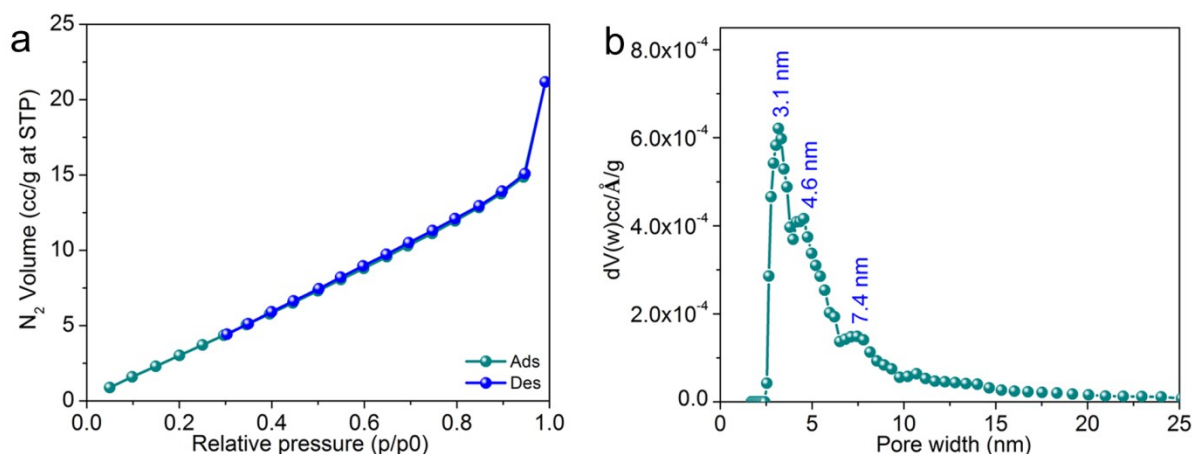


Fig. S1 a) N_2 adsorption-desorption isotherm of cerium phenylphosphonate (CPP) NSs and b) corresponding pore size distribution (PSD) curve obtained by the NLDFT model.

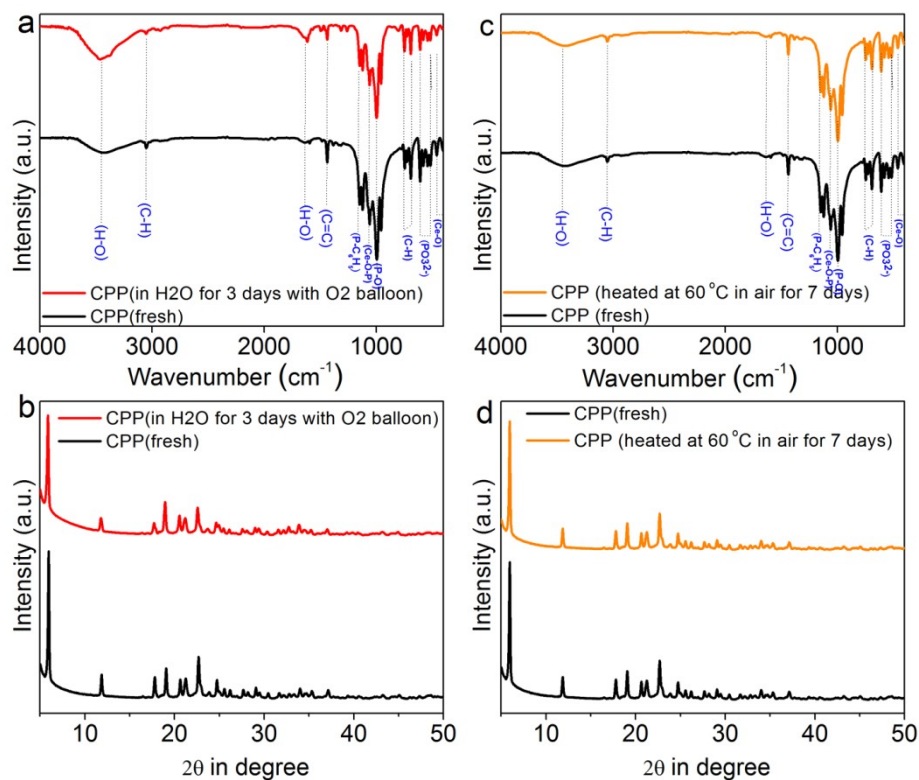


Fig. S2 Stability of catalyst in presence of O_2 a) FT IR spectra and b) powder XRD pattern before and after treatment. Stability of catalyst under air exposure c) FT IR spectra and d) powder XRD pattern before and after treatment.

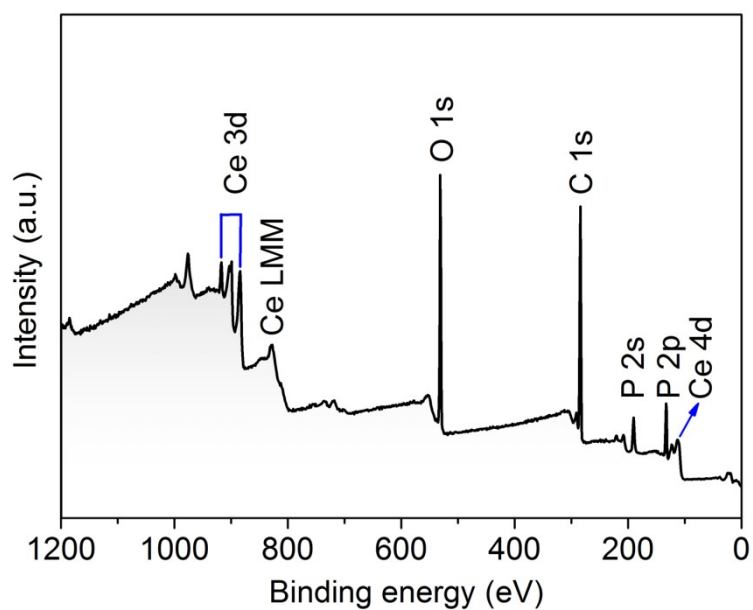


Fig. S5 XPS survey profile of cerium phenylphosphonate NSs.

Table S1: Summary of elemental Analysis of CPP NSs by EDX and XPS

Element	Ce L	P K	O K	C K
Theoretical (Atomic %)	4.76	9.53	28.57	57.14
TEM EDX (Atomic %)	5.44	10.52	27.06	56.98
XPS(Atom %)	3.27	10.11	31.63	54.99

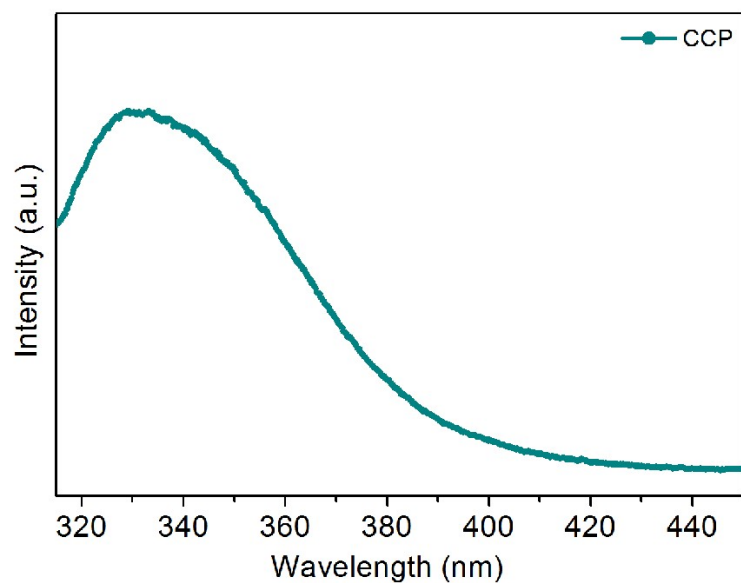


Fig. S6 Photoluminescence (PL) spectrum of cerium phenylphosphonate (CPP) NSs.

Table S2: Photoelectrochemical characterization data was obtained from the Nyquist fitted plot (Fig. 5i).

Sample	Condition	Electrolyte resistance (R_s)	Charge Transfer Resistance (R_{ct})	Constant Phase Elements (Q)	Pseudo Capacitance (C)
CPP	Dark	29.65 Ω	8143 Ω	6.063e-6 F.s ^(a-1)	4.204e-6 F
	Light	29.93 Ω	3175 Ω	10.59e-6 F.s ^(a-1)	9.405e-6 F

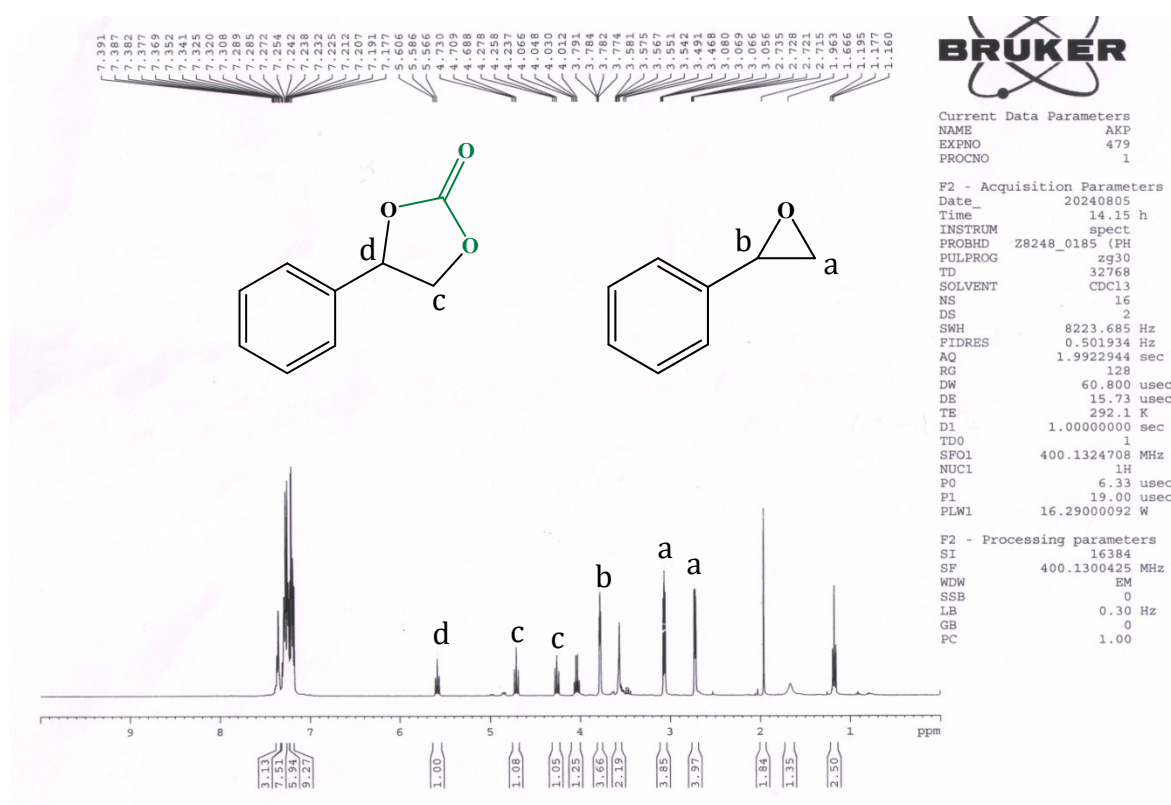


Fig. S7 ¹H NMR (400 MHz, CDCl₃) spectra of crude product of CO₂ cycloaddition reaction with styrene oxide after **3h** reaction (Fig. 6c) over CPP NSs.

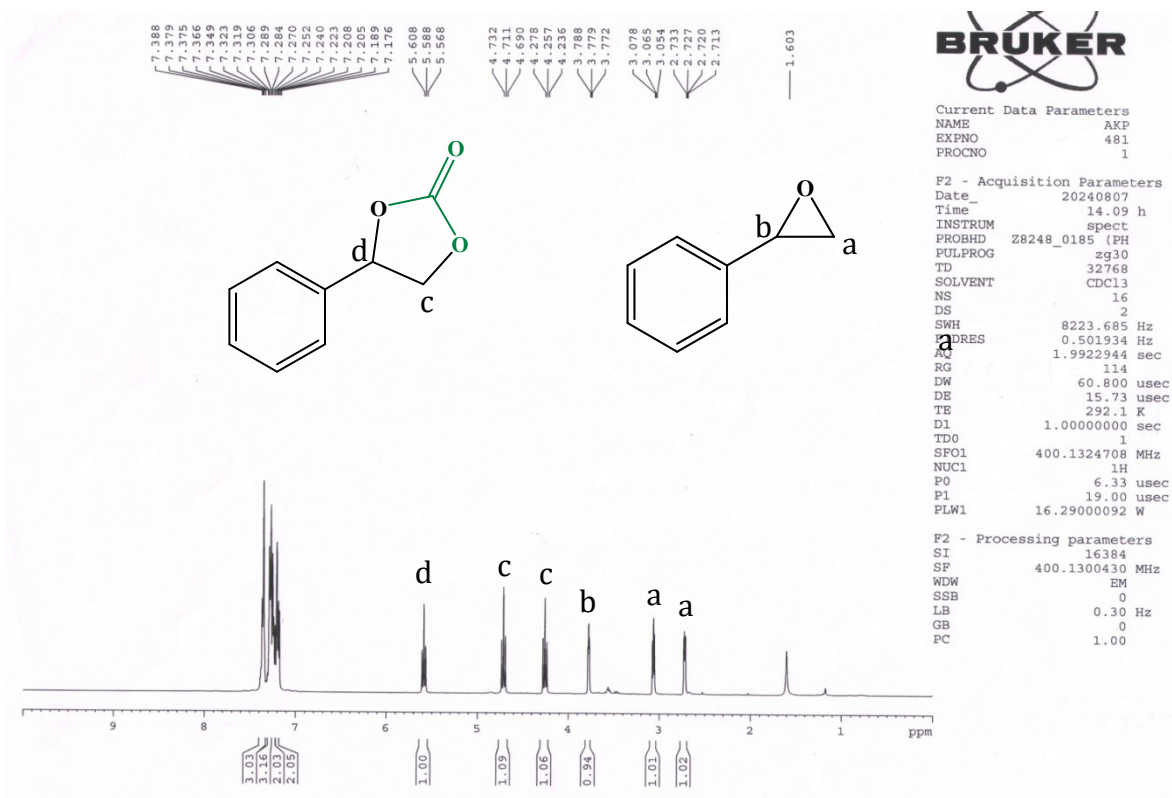


Fig. S8 ^1H NMR (400 MHz, CDCl_3) spectra of crude product of CO_2 cycloaddition reaction with styrene oxide after **6h** reaction (Fig. 6c) over CPP NSs.

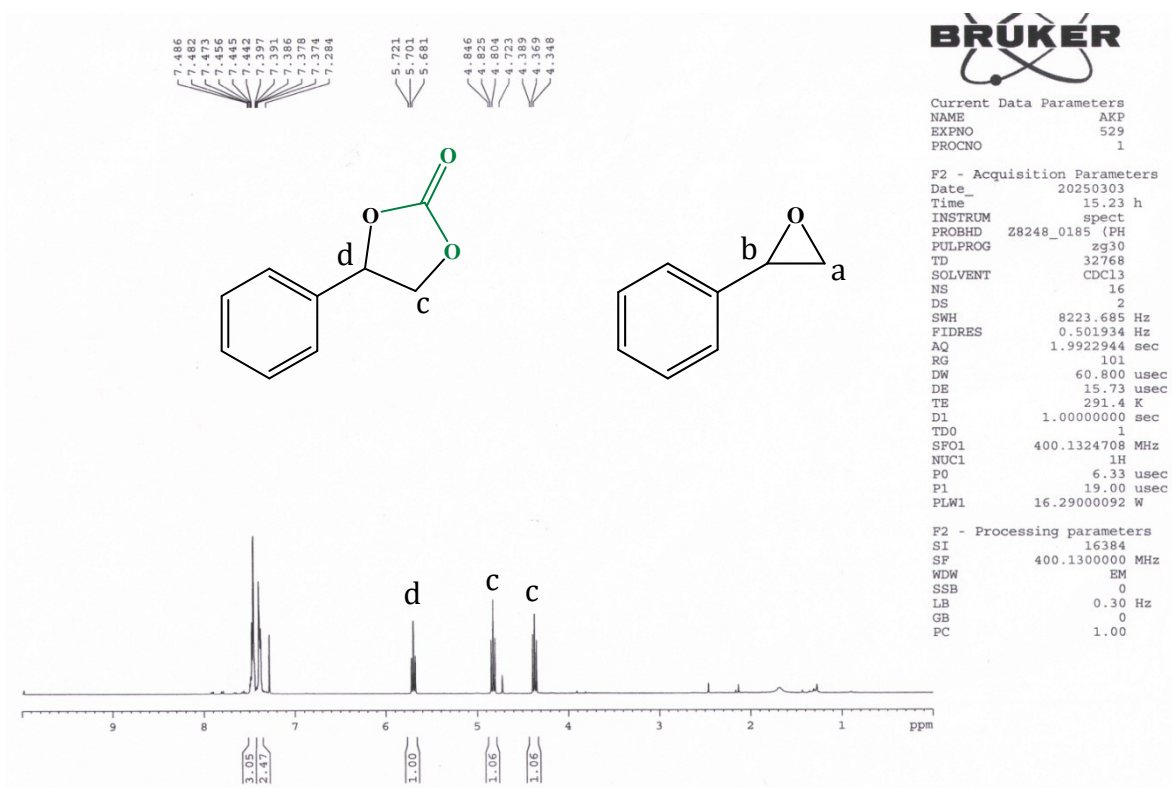


Fig. S9 ^1H NMR (400 MHz, CDCl_3) spectra of crude product of CO_2 cycloaddition reaction with styrene oxide after **12h** reaction (Fig. 6c) over CPP NSs.

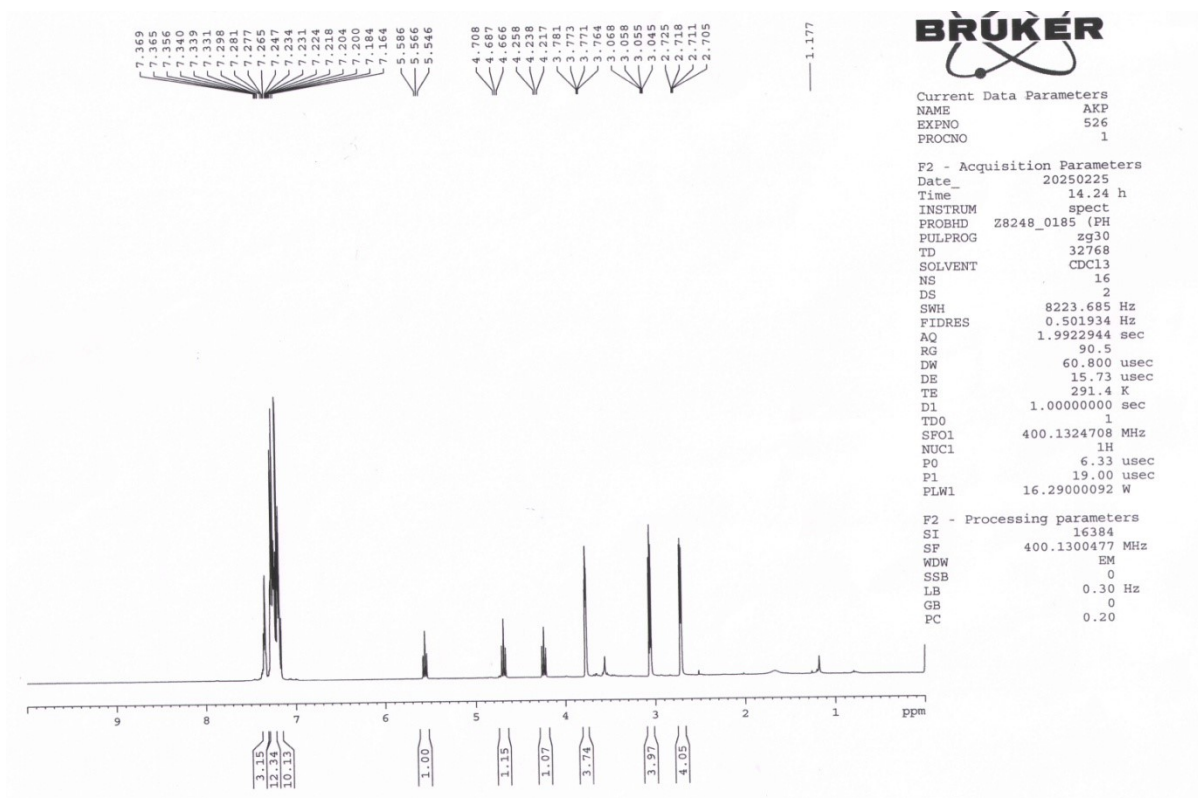


Fig. S10 ^1H NMR (400 MHz, CDCl_3) spectra of crude product of CO_2 cycloaddition reaction with styrene oxide after 12h reaction without CPP NSs (Table 2, entry 2).

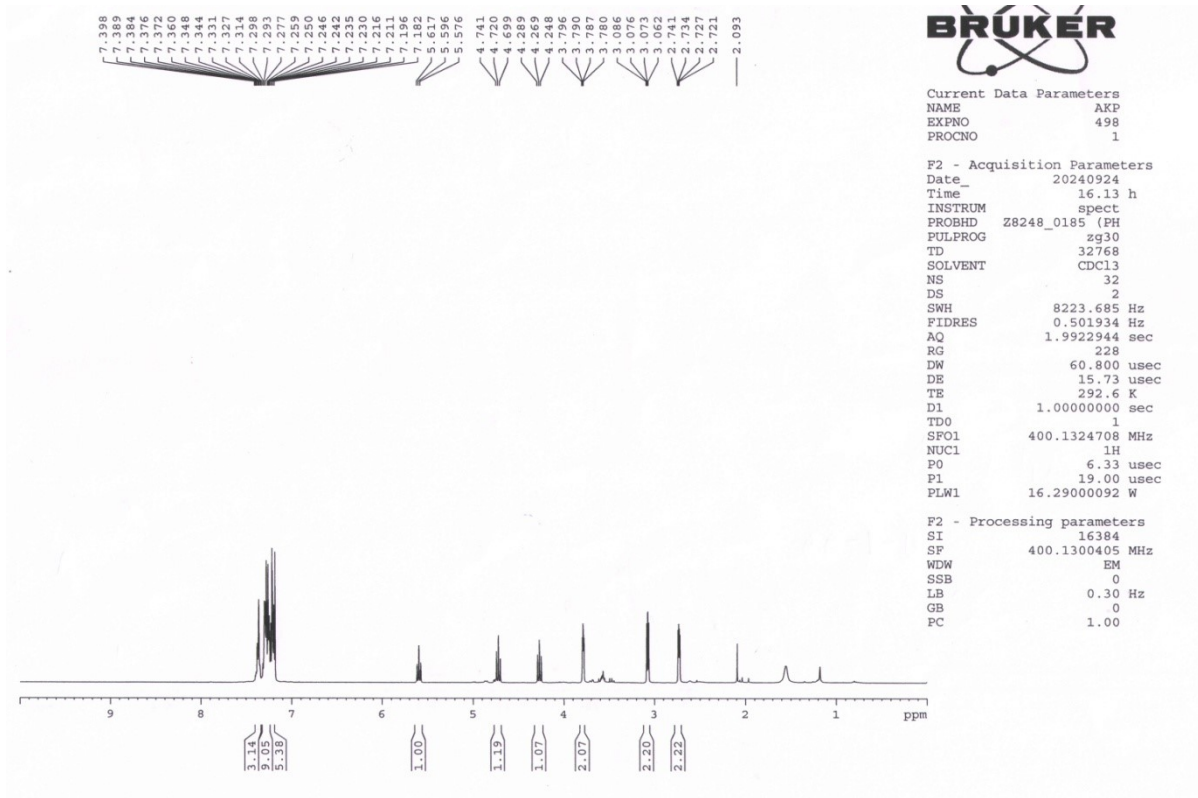


Fig. S11 ^1H NMR (400 MHz, CDCl_3) spectra of crude product of CO_2 cycloaddition reaction with styrene oxide after 12h reaction over CPP NSs without light (Table 2, entry 3).

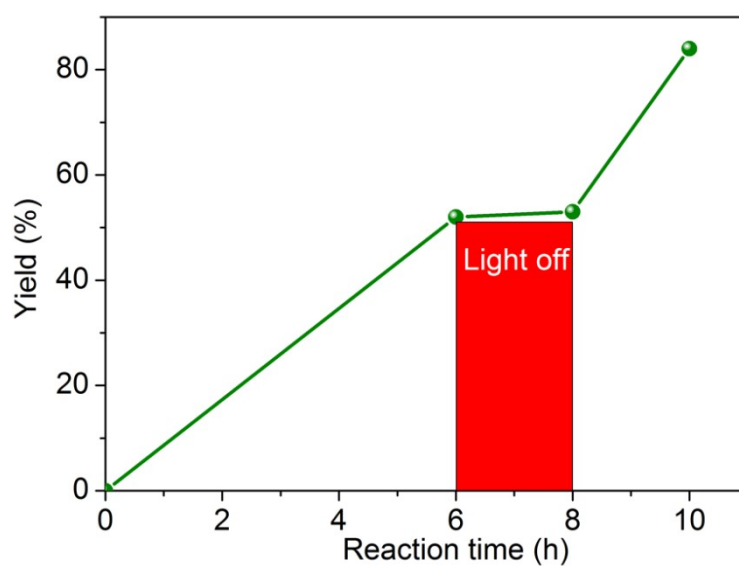


Fig. S12 light-on/light-off experiment for CO₂ cycloaddition reaction with styrene oxide over CPP NSs.

Table S3. Standard reaction was carried out in different temperature.

Entry	Variation from the standard conditions	Time (h)	Yield (%)	Rate (mmol/h)	Activity (mmol/h/g)	AQY *10 ⁵
1	Standard Condition	12	95.0	0.2375	9.5	513.9
2	25°C (Dark)	12	29.8	0.074625	2.985	161.5
3	50 °C (Dark)	12	32.6	0.0814	3.3	176.2
4	75 °C (Dark)	12	72.8	0.182	7.28	393.8

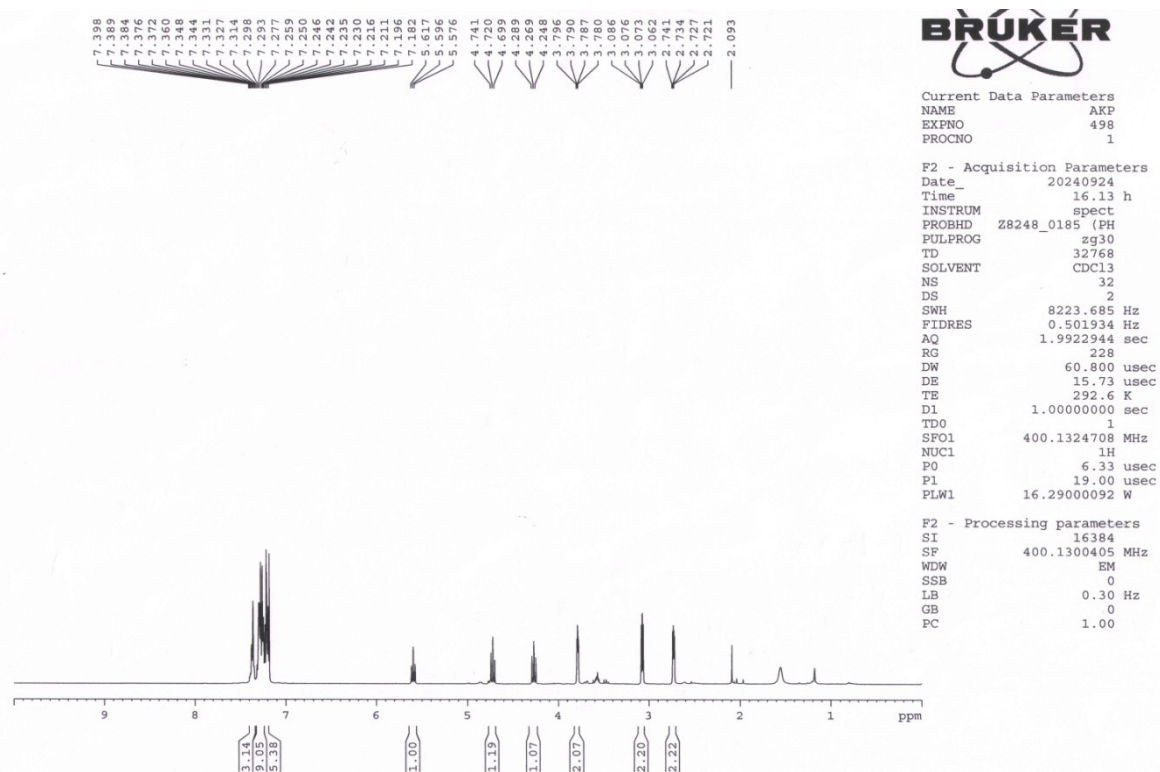


Fig. S13 ^1H NMR (400 MHz, CDCl_3) spectra of crude product of CO_2 cycloaddition reaction with styrene oxide after 12h reaction over CPP NSs at 50 °C in dark (Table S3, entry 3).

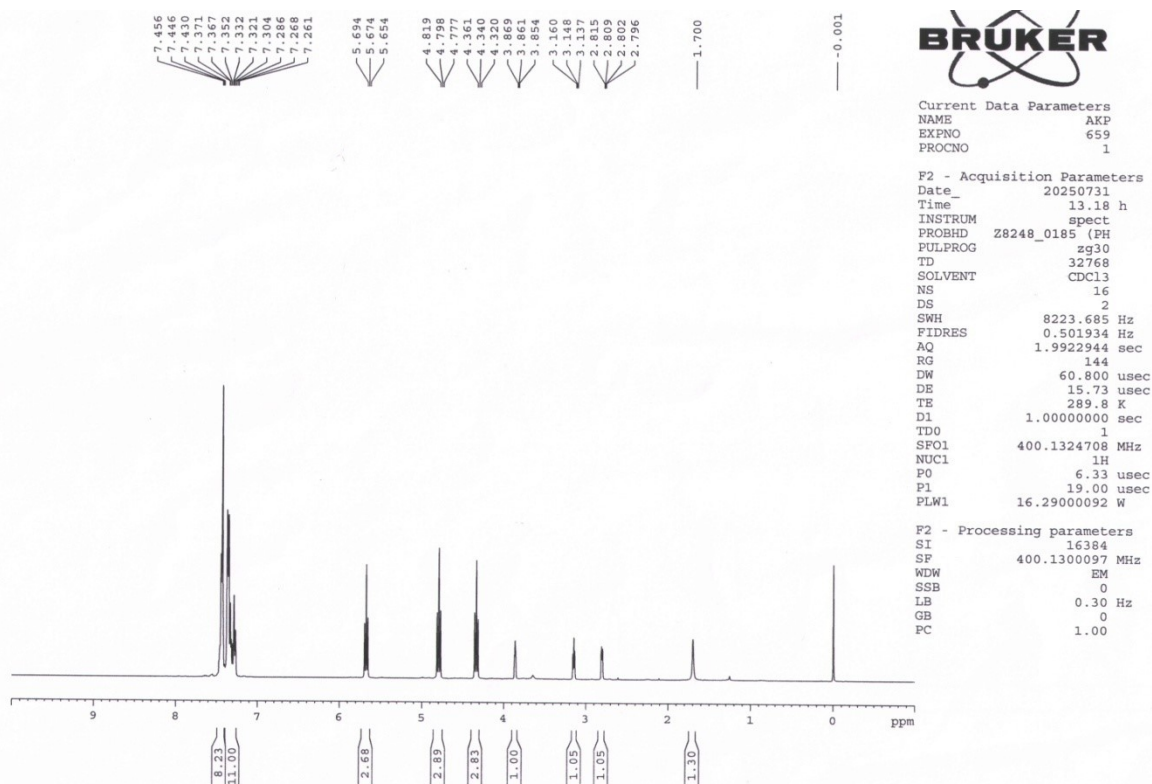


Fig. S14 ^1H NMR (400 MHz, CDCl_3) spectra of crude product of CO_2 cycloaddition reaction with styrene oxide after 12h reaction over CPP NSs at 75 °C in dark (Table S3, entry 4).

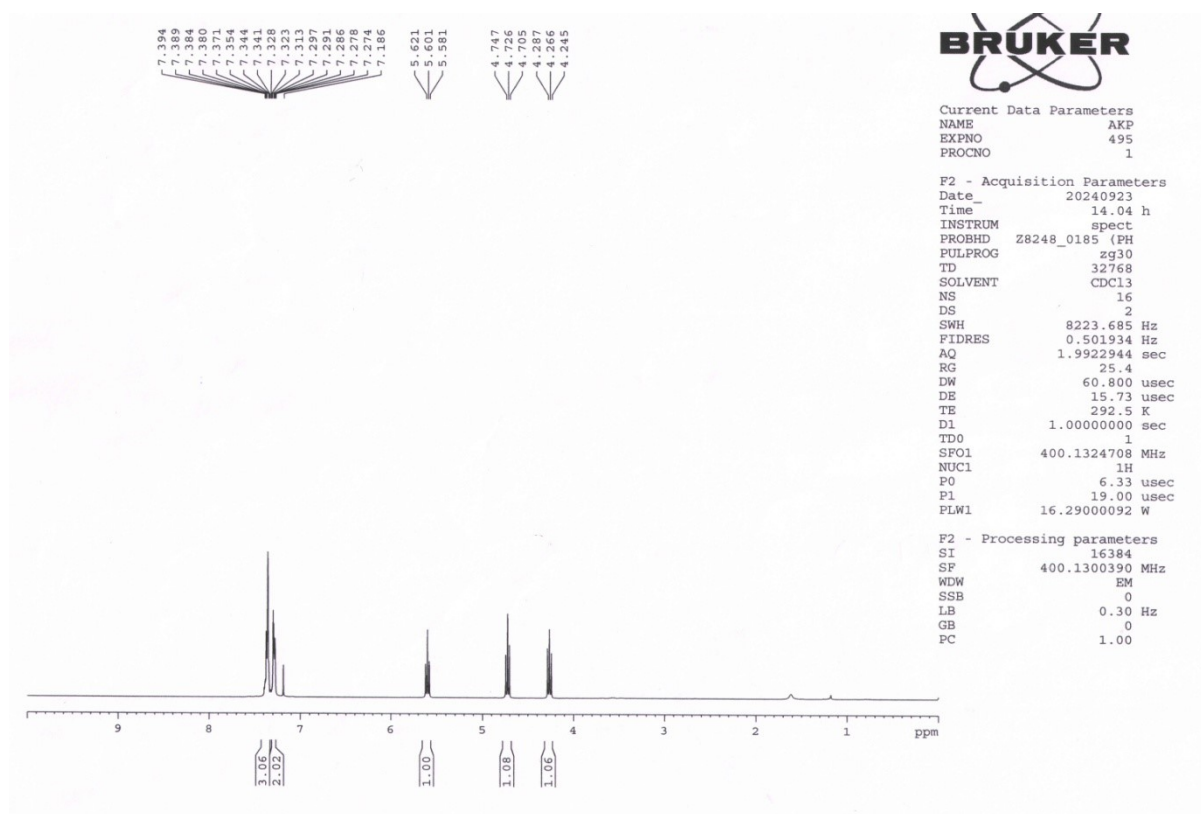


Fig. S15 ^1H NMR (400 MHz, CDCl_3) spectra of crude product of CO_2 cycloaddition reaction with styrene oxide after 12h reaction over CPP NSs without solvent (Table 2, entry 14).

Table S4: Standard reaction was carried out in presence of different amount of TBAB.

Entry	Amount of TBAB (mmol)	Time (h)	Yield (%)	Rate (mmol/h)	Activity (mmol/h/g)	AQY $\times 10^5$
1	0.3	12	95.0	0.2375	9.5	513.9
2	0.2	12	10.16	0.0254	1.016	54.9
3	0.1	12	0.0	0.0	0.0	-

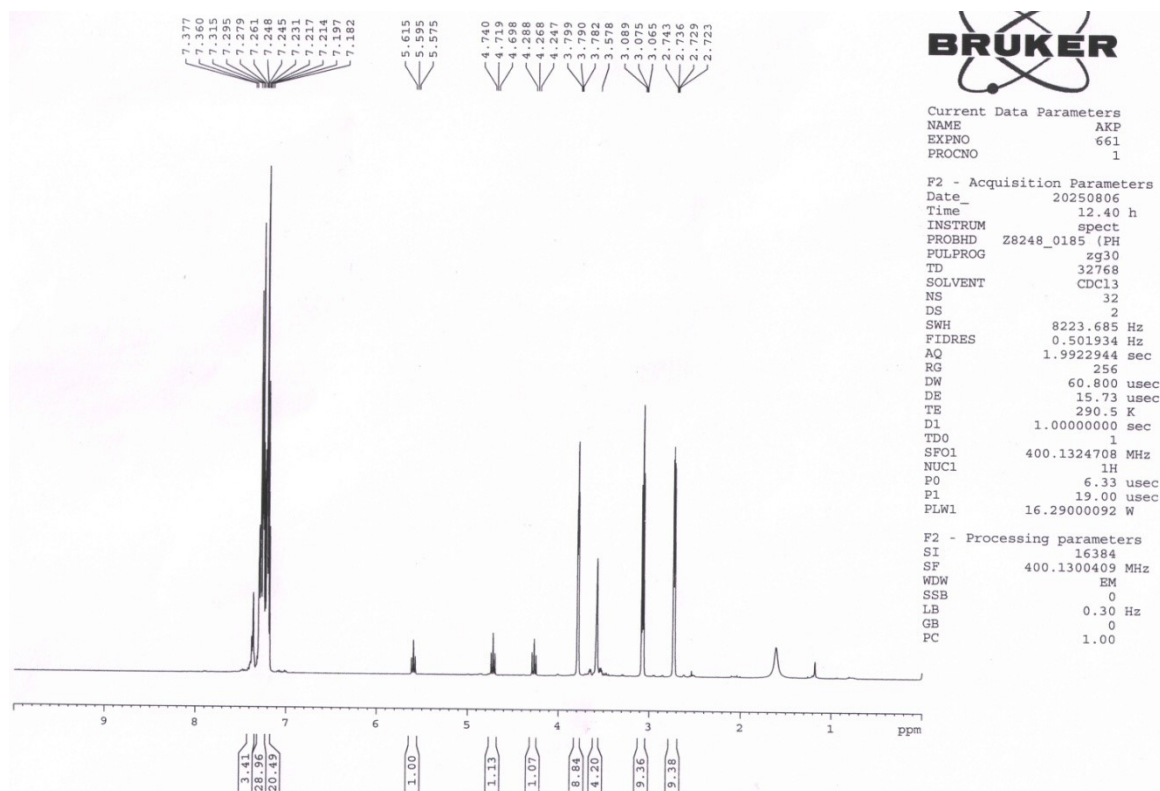


Fig. S16 ^1H NMR (400 MHz, CDCl_3) spectra of crude product of CO_2 cycloaddition reaction with styrene oxide after 12h reaction over CPP NSs with 0.2 mmol TBAB (Table S4, entry 2).

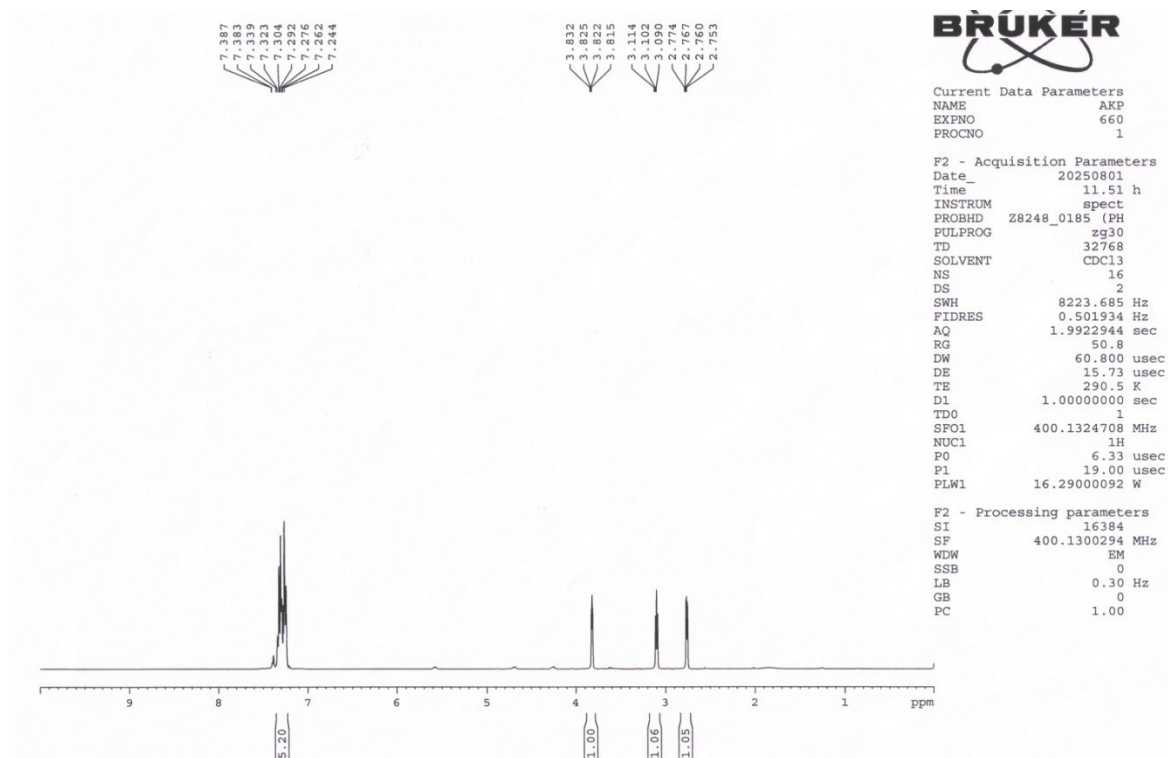


Fig. S17 ^1H NMR (400 MHz, CDCl_3) spectra of crude product of CO_2 cycloaddition reaction with styrene oxide after 12h reaction over CPP NSs with 0.1 mmol TBAB (Table S4, entry 3).

Table S5: Standard reaction was carried out in presence of different scavengers.

Entry	Variation from the standard conditions	Time (h)	Yield (%)	Rate (mmol/h)	Activity ($\mu\text{mol/h/g}$)
1	Standard condition	12	95	0.2375	9.50
2	AgNO_3 (e quencher)	12	0	0	0.00
3	Na_2EDTA (h quencher)	12	33.89	0.084725	3.389
4	DMPO (radical quencher)	12	19.41	0.048525	1.941

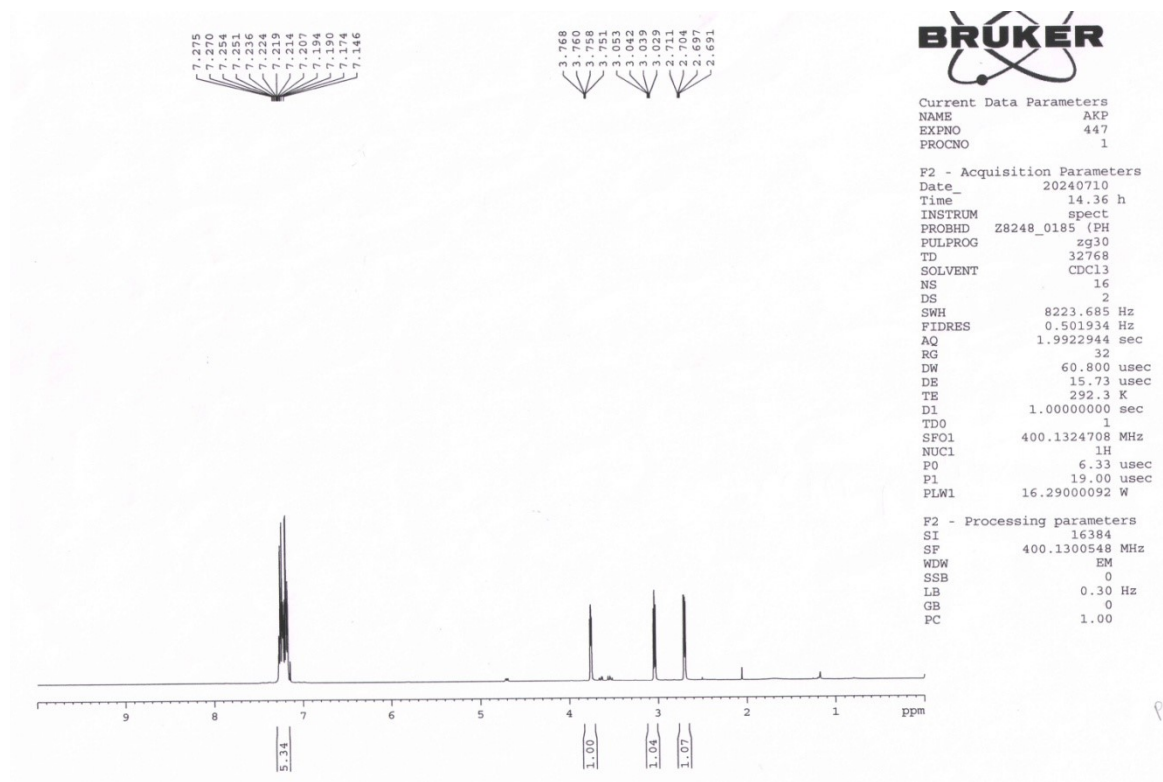


Fig. S18 ^1H NMR (400 MHz, CDCl_3) spectra of crude product. The standard reaction was carried out in presence of AgNO_3 (Table S5, entry 2).

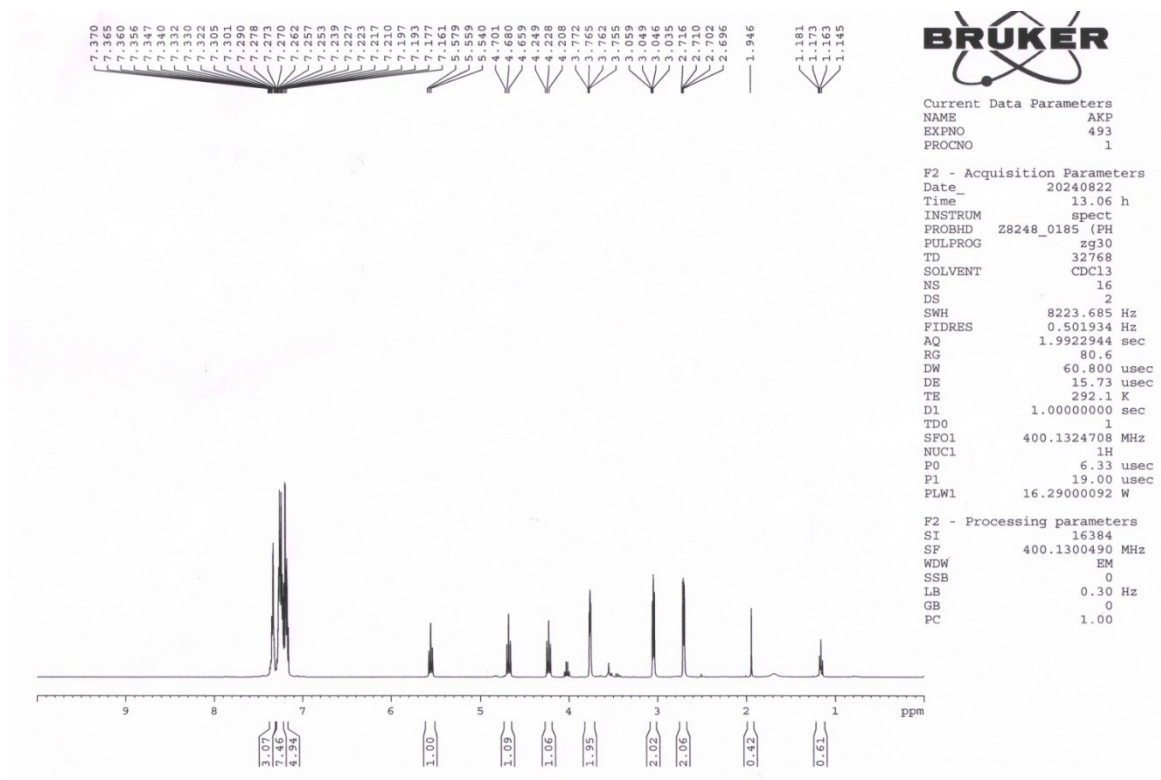


Fig. S19 ^1H NMR (400 MHz, CDCl_3) spectra of crude product. The standard reaction was carried out in presence of Na_2EDTA (Table S5, entry 3).

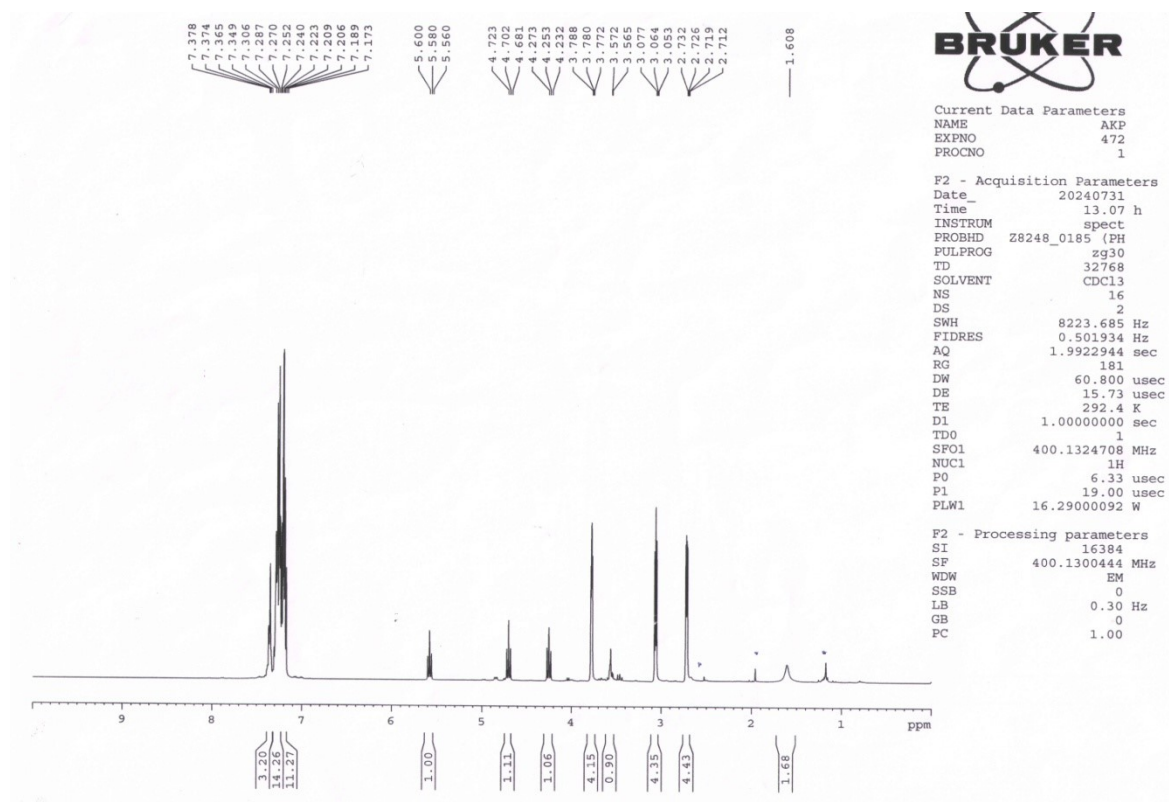


Fig. S20 ^1H NMR (400 MHz, CDCl_3) spectra of crude product. The standard reaction was carried out in presence of DMPO (Table S5, entry 4).

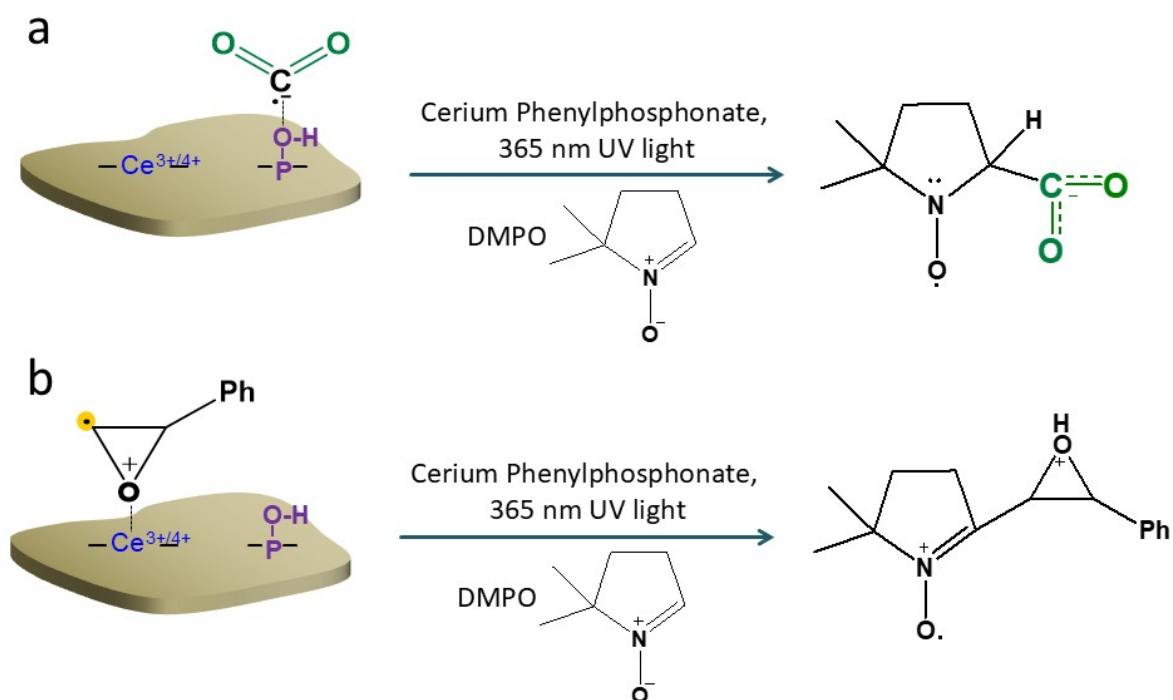


Fig. S21 Schematic diagram of a) styrene oxide radical and b) CO_2 radical intermediates trapped by DMPO.

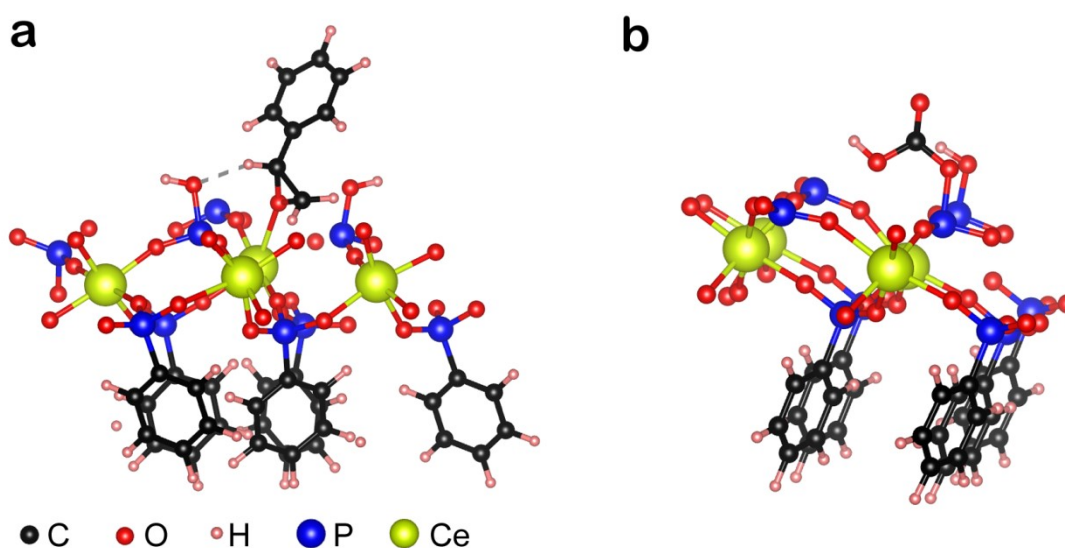


Fig. S22 DFT optimized structure of (a) styrene oxide and (b) CO_2 adsorbed crystal respectively

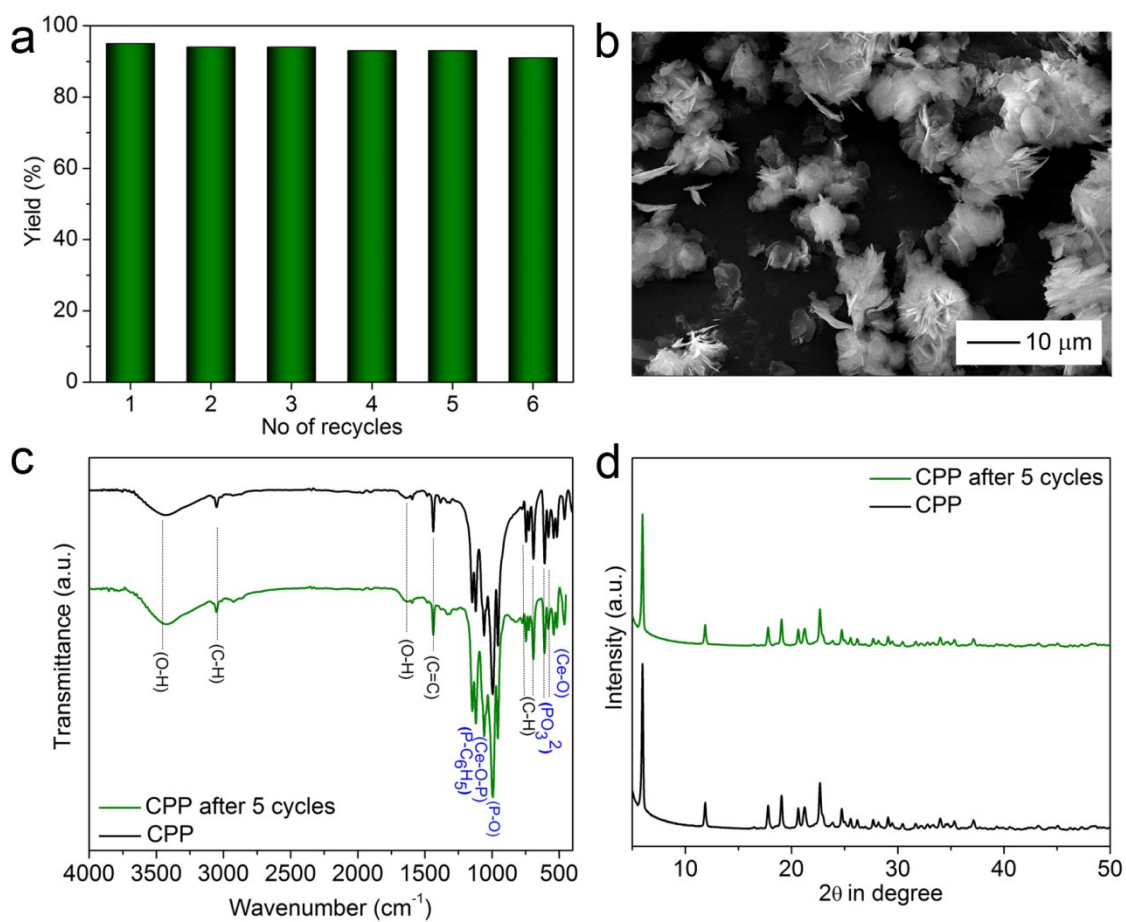


Fig. S23 a) Recyclability of CPP NSs in the standard reactions condition. b) SEM image, c) FT IR and d) powder XRD pattern of reused catalyst.

¹H and ¹³C NMR data

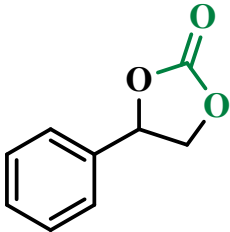
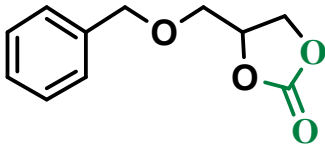
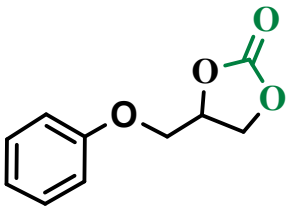
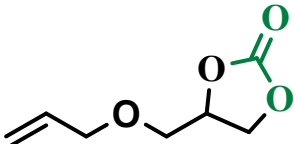
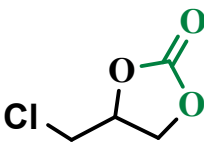
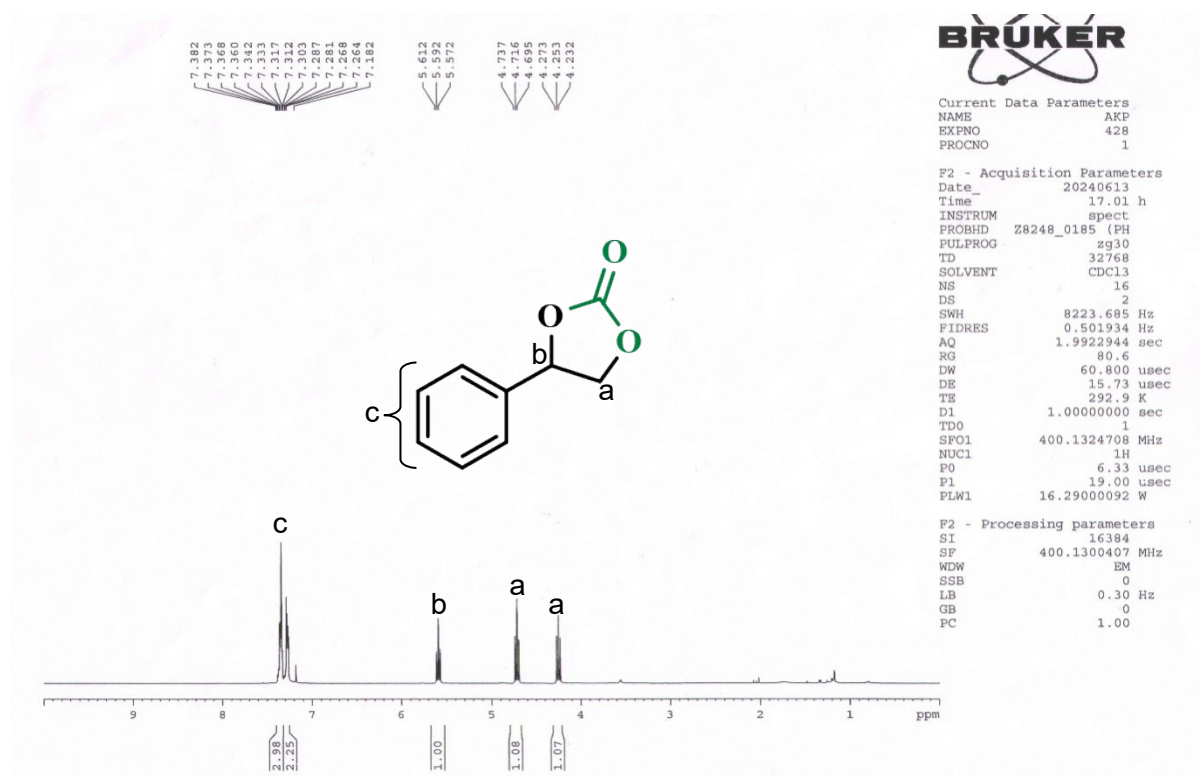
Table 3. Entry 1 Product 1.	
	4-phenyl-1, 3-dioxolan-2-one: ¹ H NMR (400MHz, CDCl ₃) δ 7.382 - 7.333 (3H, m), δ 7.317 – 7.264 (2H, m), δ 5.612 -5.572 (1H, t, J=8 Hz), δ 4.737-4.695(1H, t, J=8.4 Hz), δ 4.273-4.232(1H, t, J=8.2 Hz) ppm; ¹³ C NMR (400MHz, CDCl ₃) δ 154.83, 135.79, 129.76, 129.26, 125.88, 78, 71.17 ppm.
Table 3. Entry 2 Product 2.	
	4-((benzyloxy)methyl)-1, 3-dioxolan-2-one: ¹ H NMR (400MHz, CDCl ₃) δ 7.312 - 7.277 (2H, m), δ 7.251 - 7.223 (3H, m), δ 4.770-4.714 (1H, m), δ 4.567-4.481 (2H, dd, J=22.4 Hz,12 Hz), δ 4.431-4.389(1H, t, J=8.4 Hz), δ 4.332-4.296 (1H, dd, J=14.4 Hz,6.2 Hz), 3.658-3.621 (1H, dd, J=10.8 Hz,4 Hz), δ 3.569-3.532 (1H, dd, J = 11Hz, 3.8 Hz) ppm; ¹³ C NMR (400MHz, CDCl ₃) δ 154.97, 137.07, 128.60, 128.12, 127.78, 75.01, 73.71, 68.83, 66.31 ppm.
Table 3. Entry 3 Product 3.	
	4-((phenoxy) methyl)-1, 3-dioxolan-2-one: ¹ H NMR (400MHz, CDCl ₃) δ 7.264-7.218 (2H, m), δ 6.970 – 6.933 (1H, t, J=7.4 Hz), δ 6.854 – 6.835 (2H, d, J=7.6 Hz), δ 4.984-4.939 (1H, m), δ 4.577-4.535 (1H, t, J=8.4 Hz), 4.496-4.460 (1H, dd, J=8.4 Hz, 6 Hz), 4.195-4.157 (1H, dd, J=10.8 Hz,4.4 Hz), δ 4.106-4.070 (1H, dd, J = 10.8 Hz, 3.6 Hz) ppm; ¹³ C NMR (400MHz, CDCl ₃) δ 157.75, 154.56, 129.71, 122.05, 114.63, 74.03, 66.91, 66.26 ppm.
Table 3. Entry 4 Product 4	
	4-((allyloxy)methyl)-1, 3-dioxolan-2-one: ¹ H NMR (400MHz, CDCl ₃) δ 5.840-5.770 (1H, m), δ 5.244-5.145 (2H, m), δ 4.78 – 4.735 (1H, m), δ 4.461-4.420 (1H, t, J=8.2 Hz), δ 4.354 – 4.318 (1H, dd, J=8.4 Hz,6 Hz), 4.002-3.982 (1H, m), δ 3.649-3.612 (dd, 2H, J=10.8 Hz,4 Hz), 3.571-3.534 (dd, 2 H, J=11.2 Hz,3.6 Hz) ppm; ¹³ C NMR (400MHz, CDCl ₃) δ 154.96, 133.66, 117.98, 75.02, 72.62, 68.84, 66.30 ppm.
Table 3. Entry 5 Product 5	
	4-(chloromethyl)-1, 3-dioxolan-2-one: ¹ H NMR (400MHz, CDCl ₃) δ 4.958-4.901 (1H, m), δ 4.560– 4.517 (1H, t, J=8.6 Hz), δ 4.370-4.334 (1H, dd, J=8.8 Hz, 5.6 Hz), 3.766-3.722 (1H, dd, J = 12.2 Hz, 5.4 Hz), 3.692-3.653 (1H, dd, J=12, 3.6 Hz) ppm; ¹³ C NMR (400MHz, CDCl ₃) δ 154.26, 74.31, 66.99, 43.74 ppm.

Table 3. Entry 1 Product 1.

^1H NMR (400 MHz, CDCl_3)



^{13}C NMR (400 MHz, CDCl_3)

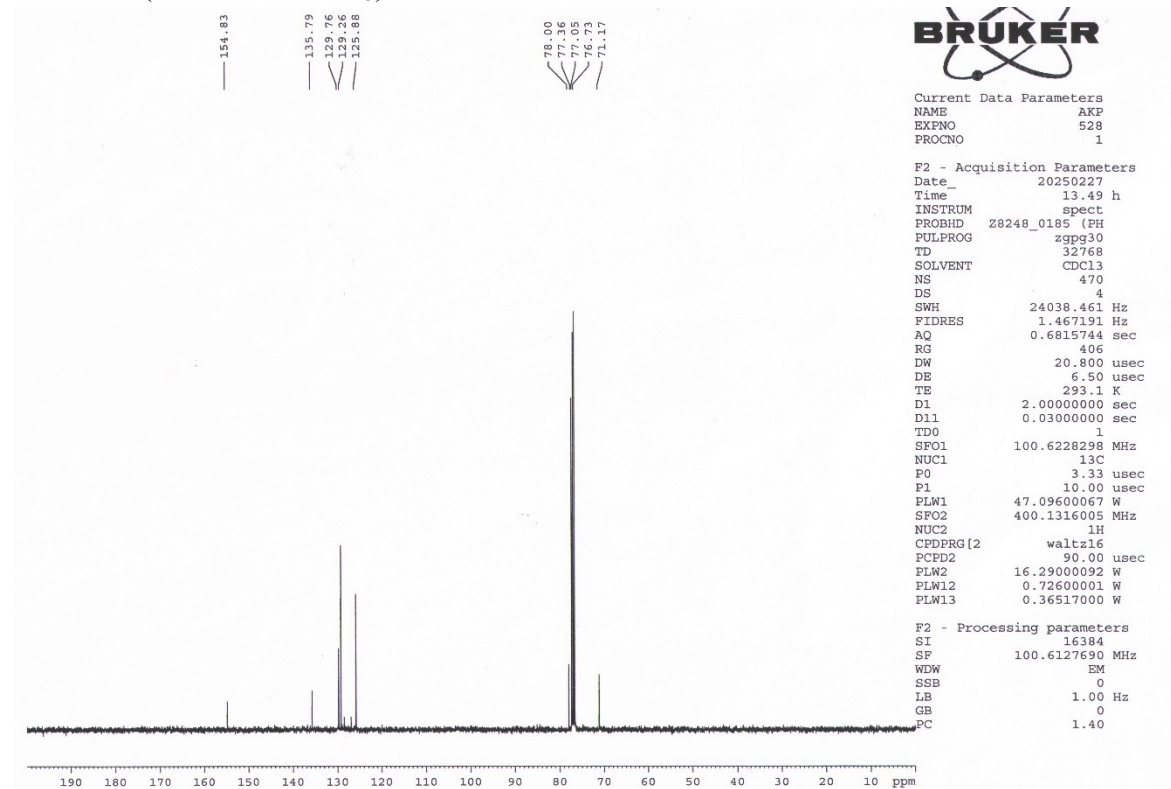
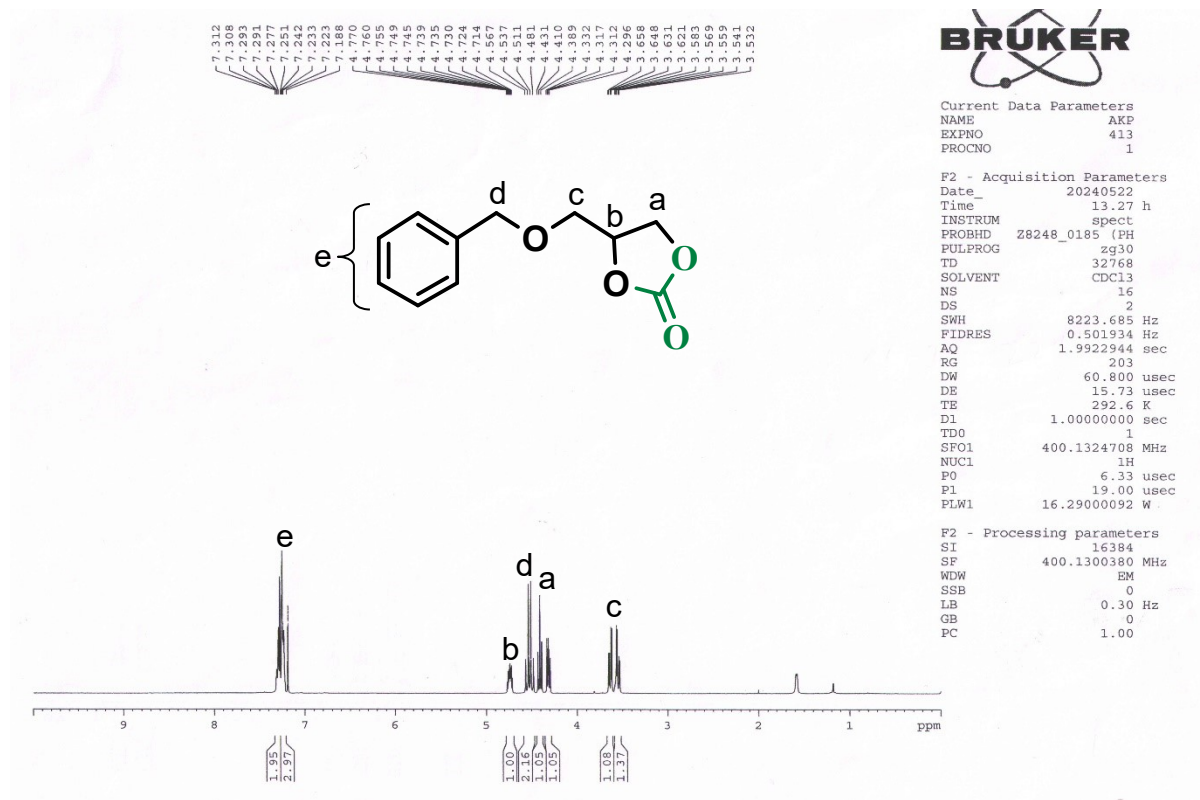


Table 3. Entry 2 Product 2.

^1H NMR (400 MHz, CDCl_3)



^{13}C NMR (400 MHz, CDCl_3)

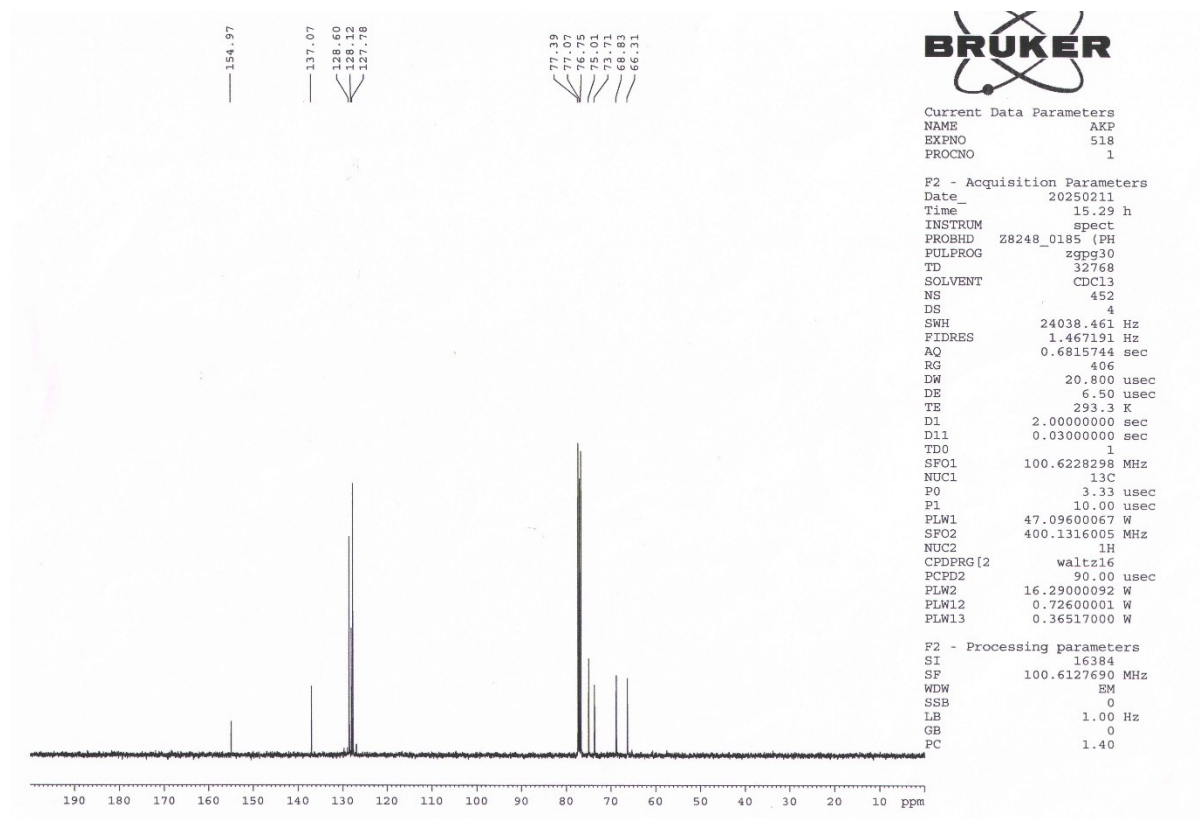
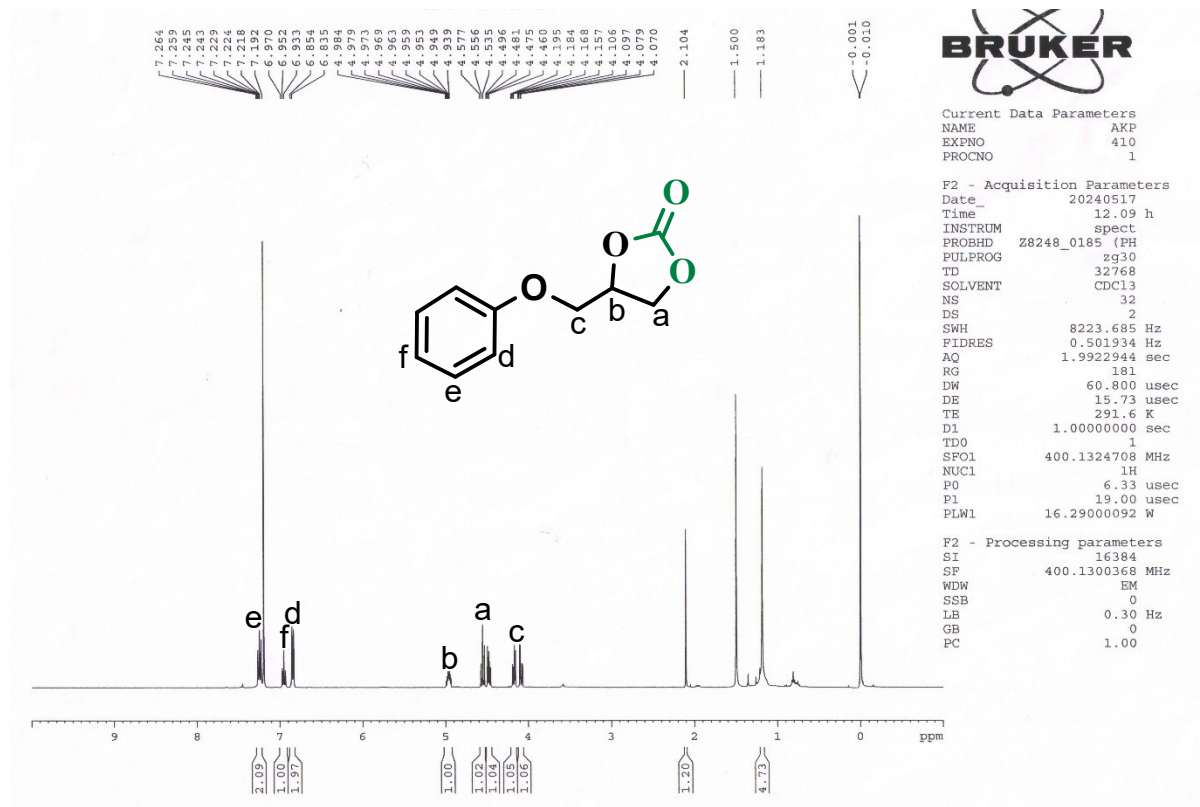


Table 3. Entry 3 Product 3.

^1H NMR (400 MHz, CDCl_3)



^{13}C NMR (400 MHz, CDCl_3)

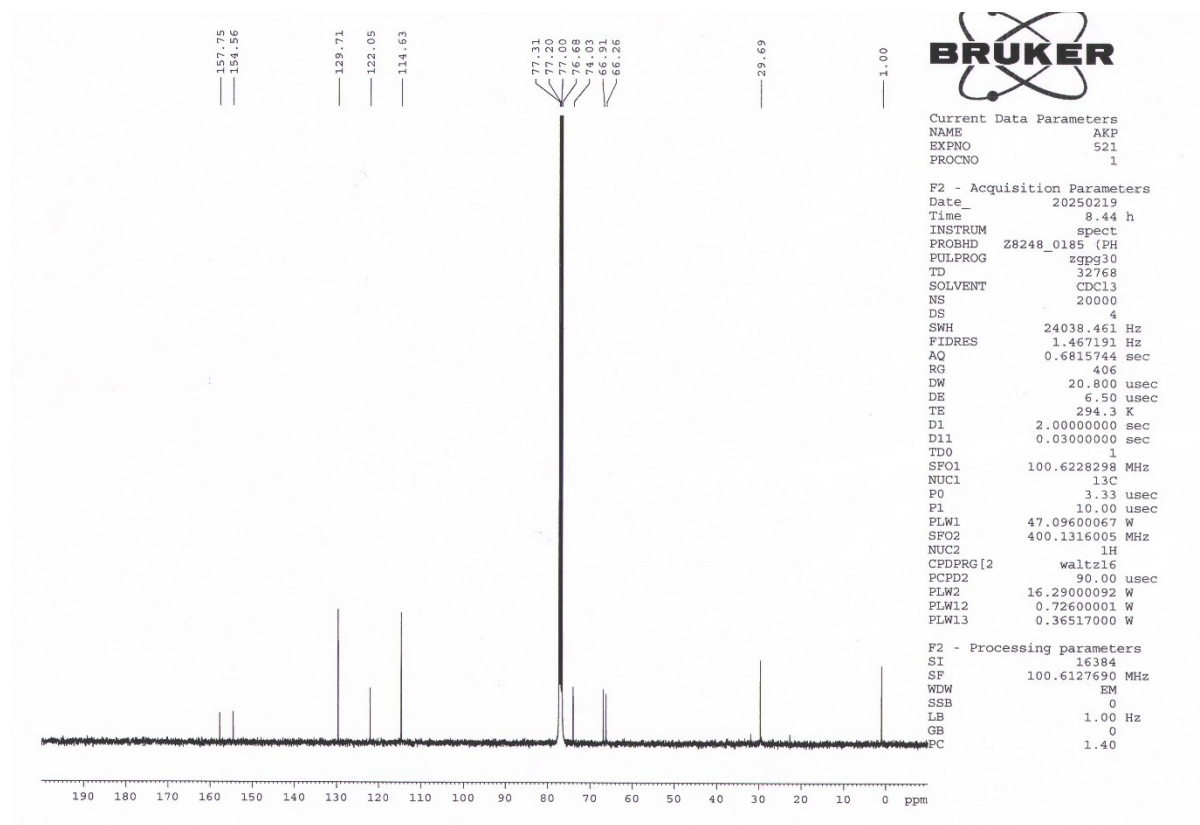
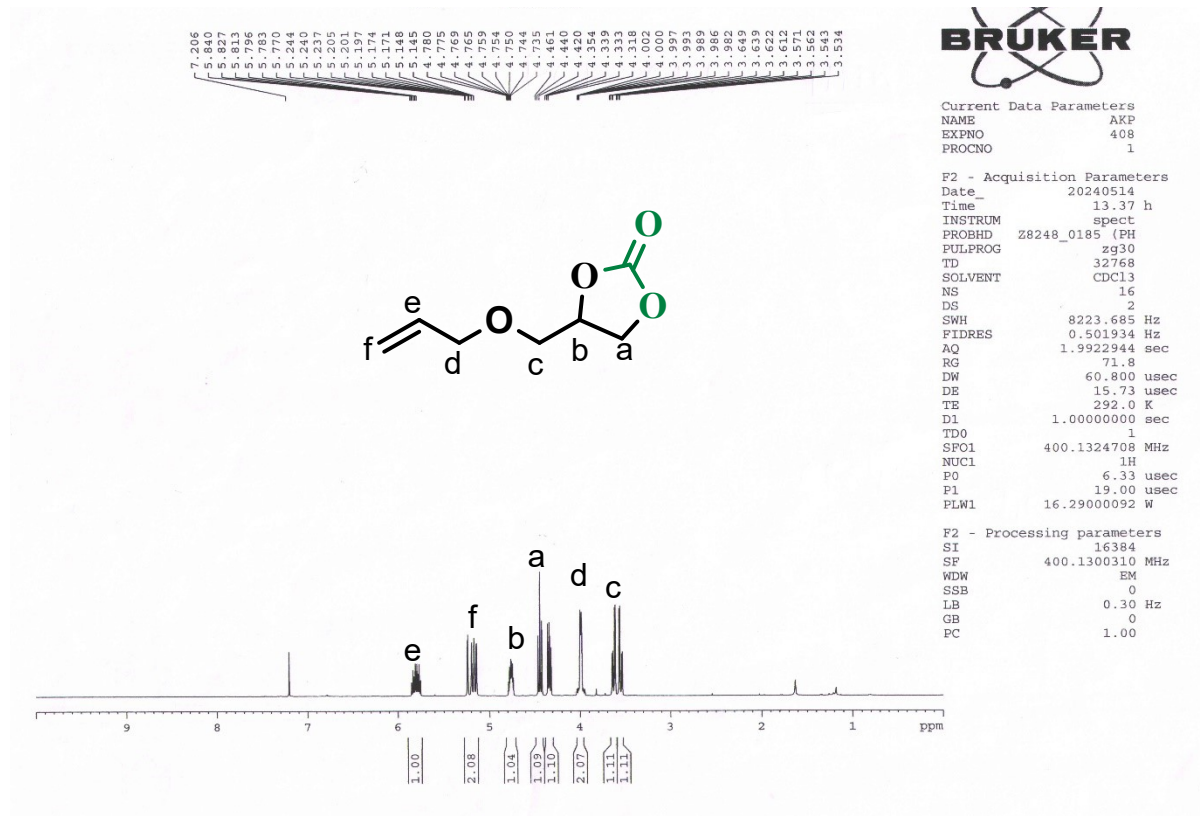


Table 3. Entry 4 Product 4.

^1H NMR (400 MHz, CDCl_3)



^{13}C NMR (400 MHz, CDCl_3)

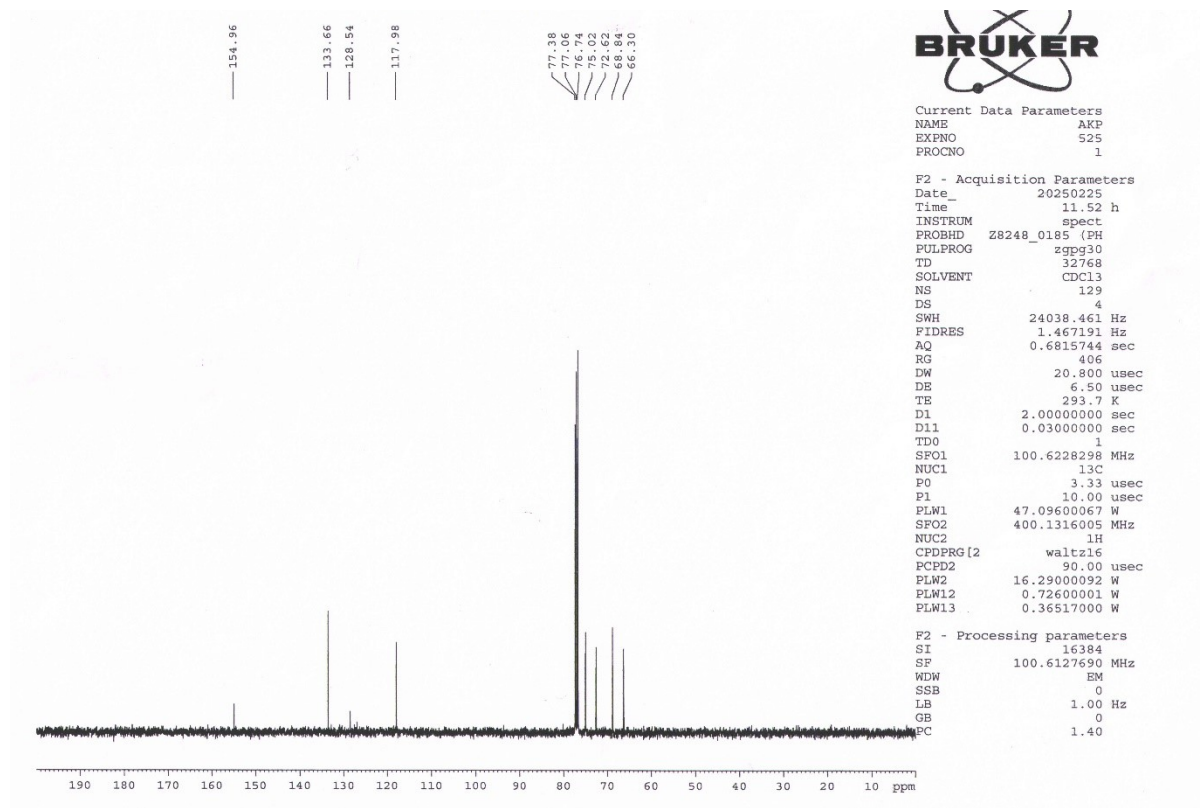
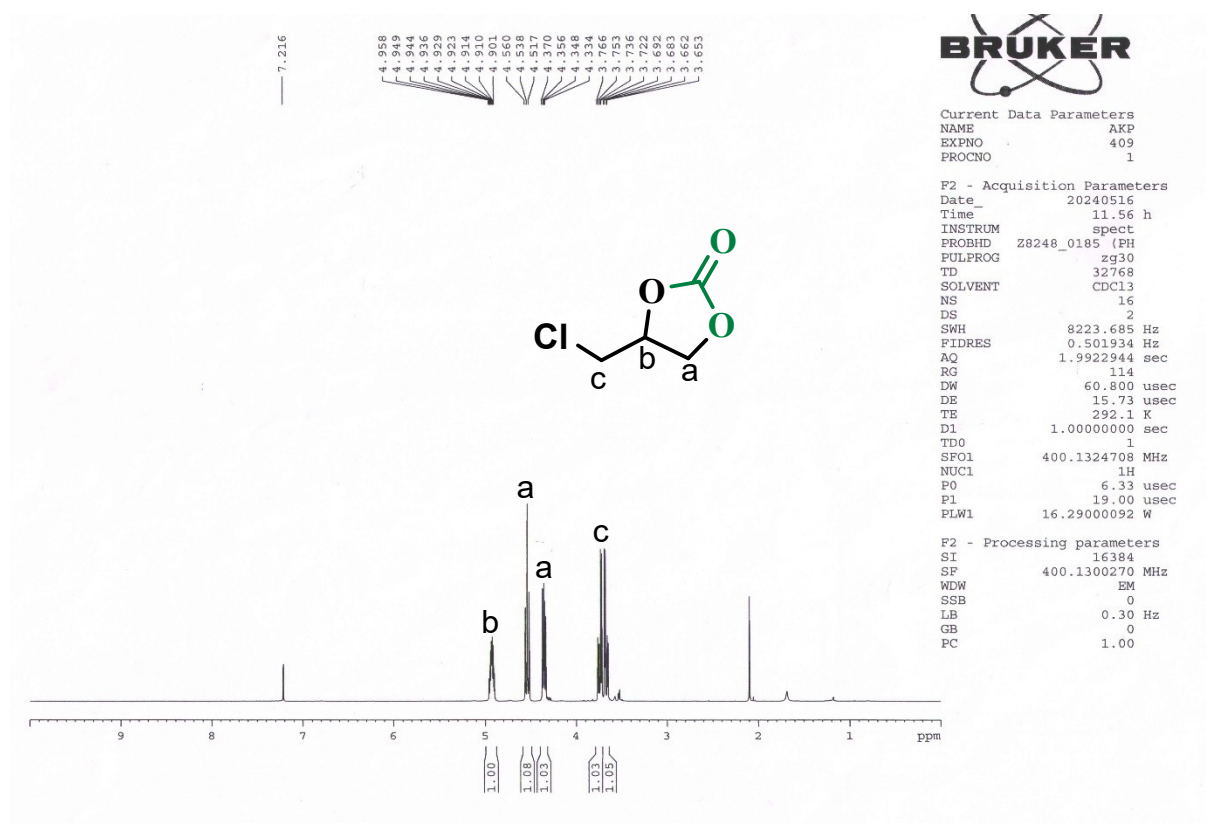


Table 3. Entry 5 Product 5.

^1H NMR (400 MHz, CDCl_3)



^{13}C NMR (400 MHz, CDCl_3)

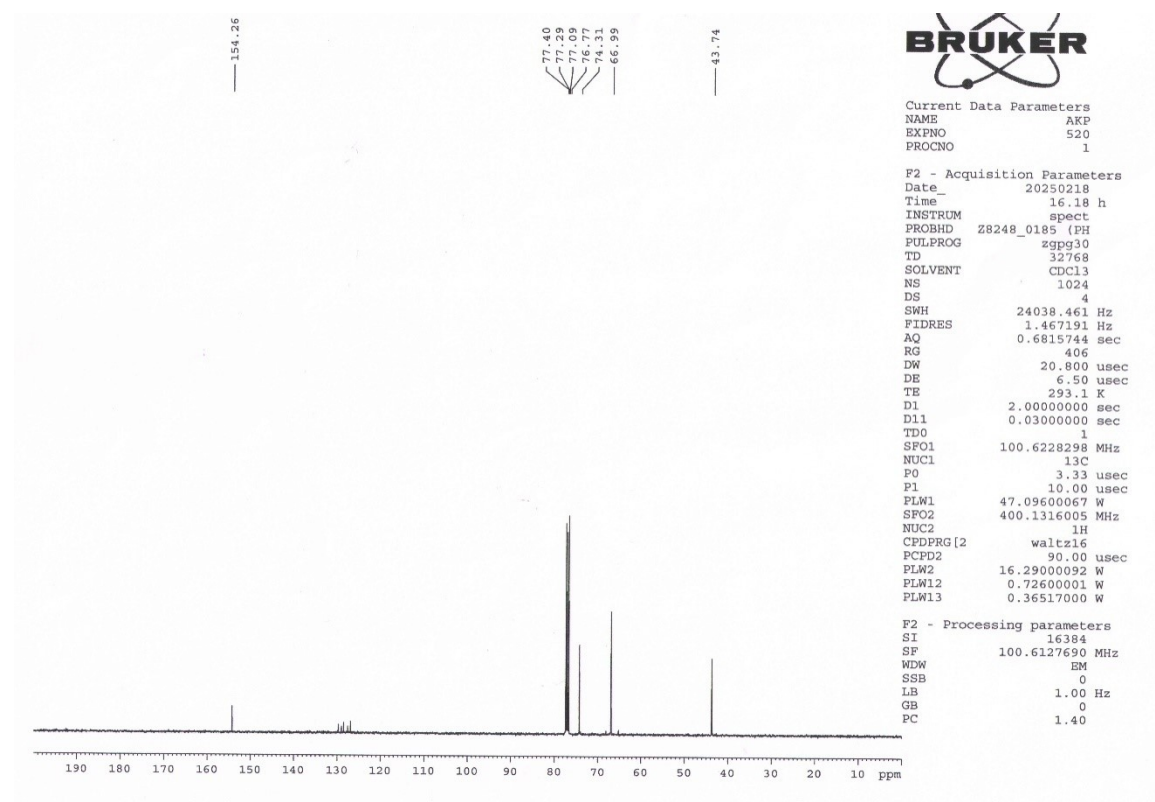


Table S6: Comparison of the reaction yield of allylglycidyl ether over different catalysts.

Entry	Catalyst name	Reaction Condition	Yield (%)	Reference
1.	4,4''-diamino-p-terphenyl (DT)	Allyl glycidyl ether (5 mmol), TBAB (2.5 mol%), 1 atm CO ₂ , 0.7 mol% catalyst, blue LEDs (λ =450–455 nm, 6 W light intensity), RT, 6 h., Photocatalytic.	96	<i>Appl. Catal. A Gen.</i> 2025, 698 , 120249
2.	Al ₂ O ₃ /CoAl ₂ O ₄	Allyl glycidyl ether (5 mmol); TBAI (0.1 mmol); 15% Co–Al ₂ O ₃ (10 mg); CO ₂ , temp (27 °C), Photocatalytic.	58	<i>Inorg. Chem.</i> 2025, 64 , 1808–1820
3.	Calix[6]arene-functionalized titanium-oxo clusters	Allyl glycidyl ether (4.0 mmol), TBAB(0.30 mmol), CO ₂ (1 atm), catalyst (15 mg), RT, 10 W 430 nm LED, 20 h., Photocatalytic.	99	<i>Inorg. Chem. Front.</i> , 2024, 11 , 3755–3764
4.	Cerium phenylphosphonate (CPP)	Allyl glycidyl ether (3 mmol), catalyst (25 mg), PEG 600 (2 mL), TBAB (0.3 mmol), CO ₂ 365 nm light (8 Watt), 12 h., Photocatalytic.	90	This work

Table S7: Comparison of the reaction yield of benzyl glycidyl ether over different catalysts.

Entry	Catalyst name	Reaction Condition	Yield (%)	Reference
1.	4,4''-diamino-p-terphenyl (DT)	Benzyl glycidyl ether (5 mmol), TBAB (2.5 mol%), 1 atm CO ₂ , catalyst (0.7 mol%), blue LEDs (λ =450–455 nm, 6 W light intensity), RT, 6 h., Photocatalytic.	76	<i>Appl. Catal. A Gen.</i> 2025, 698 , 120249
2.	Calix[6]arene-functionalized titanium-oxo clusters	Benzyl glycidyl ether (4.0 mmol), TBAB(0.30 mmol), CO ₂ (1 atm), catalyst (15 mg), RT, 10 W 430 nm LED, 20 h., Photocatalytic.	90	<i>Inorg. Chem. Front.</i> , 2024, 11 , 3755–3764
3.	Cerium phenylphosphonate (CPP)	Benzyl glycidyl ether (3 mmol), catalyst (25 mg), PEG 600 (2 mL), TBAB (0.3 mmol), CO ₂ 365 nm light (8 Watt), 12 h., Photocatalytic.	92	This work

Table S8: Comparison of the reaction yield of epichlorohydrin over different catalysts.

Entry	Catalyst name	Reaction Condition	Yield (%)	Reference
1.	4,4''-diamino-p-terphenyl (DT)	Epichlorohydrin (5 mmol), 2.5 mol% TBAB, 1 atm CO ₂ , 0.7 mol% catalyst, blue LEDs (λ =450–455 nm, 6 W), RT, 6 h., Photocatalytic.	95	<i>Appl. Catal. A Gen.</i> 2025, 698 , 120249
2.	ZnV ₂ O ₆ @Bi ₂ WO ₆ nanocomposite	epichlorohydrin (0.1 mmol), TBAB (0.1 mmol), photocatalyst (20 mg), CO ₂ , solvent, 350 W Xe lamp with a 420 nm cut-off filter, Photocatalytic.	95	<i>J. Environ. Sci.</i> 2025, 154 , 665–677
3.	Nanoflower Fe-base complex (Fe@NTC)	Epichlorohydrin (5 mL), TBAB (0.1 g), 30 mg of catalyst, CO ₂ , atmospheric pressure, 80 °C, UV light (250 W), Photo-thermal.	84	<i>J. Environ. Chem. Eng.</i> 2024, 12 , 112544
4.	Al ₂ O ₃ /CoAl ₂ O ₄	Epichlorohydrin (5 mmol); TBAI (0.1 mmol, 36.5 mg); 15% Co–Al ₂ O ₃ (10 mg); CO ₂ , temp (27 °C), Photocatalytic.	79	<i>Inorg. Chem.</i> 2025, 64 , 1808–1820
5.	Bisingle-atom supported on ZnO nanosheet (Bi1/ZnO) as	Epichlorohydrin (0.61 mmol), TBAB (5 mg), DMF (2 mL), 1 bar CO ₂ , catalyst (10 mg), 300 W xenon lamp with a standard AM 1.5 G filter, 12 h., Photocatalytic.	87	<i>Sci. China Chem.</i> 2024, 67 , 2292–2299.
6.	Co@BiPy-POP(M-POP)	Epichlorohydrin (0.5 mL), cocatalyst (160 mg), Photocatalyst (30 mg), CO ₂ 1 atm; blue LED light, Photocatalytic.	81	<i>Small</i> 2024, 20 , 2305307
7.	Calix[6]arene-functionalized titanium-oxo clusters	Epichlorohydrin (4.0 mmol), TBAB (0.30 mmol), CO ₂ (1 atm), catalyst (15 mg), RT, 10 W, 430 nm LED, 20 h., Photocatalytic.	99	<i>Inorg. Chem. Front.</i> , 2024, 11 , 3755–3764
8.	FeCo@BPDC	Epichlorohydrin (5 mL), TBAB (0.5 mmol), CO ₂ (1 atm), 70 °C, UV, solvent free, Photo-thermal.	92	<i>Catal. Sci. Technol.</i> , 2024, 14 , 3201–3210
9.	Cerium phenylphosphonate (CPP)	Epichlorohydrin (3 mmol), catalyst (25 mg), PEG 600 (2 mL), TBAB (0.3 mmol), CO ₂ (1 atm) 365 nm light (8 Watt), 12 h., Photocatalytic.	87	This work

Table S9: Comparison of the reaction yield of phenyl glycidyl ether over different catalysts.

Entry	Catalyst name	Reaction Condition	Yield (%)	Reference
1.	4,4''-diamino-p-terphenyl (DT)	Phenyl glycidyl ether (5 mmol), TBAB (2.5 mol%), 1 atm CO ₂ , catalyst (0.7 mol%), blue LEDs (λ =450–455 nm, 6 W), RT, 6 h., Photocatalytic.	94	<i>Appl. Catal. A Gen.</i> 2025, 698 , 120249
2.	Al ₂ O ₃ /CoAl ₂ O ₄	Phenyl glycidyl ether (5 mmol), TBAI (0.1 mmol, 36.5 mg), 15% Co–Al ₂ O ₃ (10 mg); CO ₂ , temp (27 °C), Photocatalytic.	75	<i>Inorg. Chem.</i> 2025, 64 , 1808–1820
3.	Bi-single-atom supported on ZnO nanosheet (Bi/ZnO)	Phenyl glycidyl ether(0.61 mmol), TBAB (5 mg), DMF (2 mL), 1 bar CO ₂ , catalyst (10 mg), 300 W xenon lamp with a standard AM 1.5 G filter, 12 h., Photocatalytic.	71	<i>Sci. China Chem.</i> 2024, 67 ,2292–2299.
4.	Calix[6]arene-functionalized titanium-oxo clusters	Phenyl glycidyl ether (4.0 mmol), TBAB (0.30 mmol), CO ₂ (1 atm), catalyst (15 mg), RT, 10 W 430 nm LED, 20 h., Photocatalytic.	96	<i>Inorg. Chem. Front.</i> , 2024, 11 , 3755–3764
5.	Cerium phenylphosphonate (CPP)	Phenyl glycidyl ether (3 mmol), catalyst (25 mg), PEG 600 (2 mL), TBAB (0.3 mmol), 1 atmCO ₂ , 365 nm light (8 Watt), 12 h. Photocatalytic.	90	This work

Table S10: Comparison of the reaction yield of styrene oxide over different catalysts.

Entry	Catalyst name	Reaction Condition	Yield (%)	Reference
1.	4,4''-diamino-p-terphenyl (DT)	Styrene oxide (5 mmol), TBAB (2.5mol%), 1atm CO ₂ , catalyst (0.7 mol%), blue LEDs (λ =450–455 nm, 6 W), RT, 6 h., photocatalytic.	48	<i>Appl. Catal. A Gen.</i> 2025, 698 , 120249
2.	Oxygen vacancy-rich defective tungsten oxide (WO _{3-x}) modified by Prussian blue	Styrene oxide (5 mL), TBAB (36 mg), CO ₂ , 30 mg catalyst, 300 W xenon lamp, 8 h irradiation, photo thermal.	94	<i>J. Colloid Interface Sci.</i> 2025, 683 , 807–816
3.	BiHoO ₃	Styrene oxide (1.429 mmol), ⁿ Bu ₄ NBr (9 mg, 0.028 mmol, 0.045 mmol carbon dioxide, photocatalyst (10 mg), RT, light, 24 h., photocatalytic.	98	<i>J. Solid State Chem.</i> 2024, 329 , 124359
4.	FeO _x modified defective graphitic carbon nitride composite	10 mL DMF solution of Styrene oxide (concentration of 1 mol L ⁻¹), 36 mg of TBAB, 30 mg of catalyst, 1 bar CO ₂ and ambient temperature, 300 W xenon lamp equipped with AM 1.5 filter, 12 h, photocatalytic.	99	<i>Appl. Catal. B Environ.</i> 2024, 352 , 124024
5.	ZnV ₂ O ₆ @Bi ₂ WO ₆ nanocomposite	Styrene oxide (0.1 mmol), TBAB (0.1 mmol), photocatalyst (20 mg), 1 atm CO ₂ , solvent, 350 W Xe lamp with a 420 nm cut-off filter, photocatalytic.	97	<i>J. Environ. Sci.</i> 2025, 154 , 665–677
6.	Nanoflower Fe-base complex (Fe@NTC)	Styrene oxide (5 mL), cocatalyst TBAB (0.1 g), catalyst (30 mg), 1 atm CO ₂ , 80 °C, UV light (250 W), photo-thermal.	33	<i>J. Environ. Chem. Eng.</i> 2024, 12 , 112544
7.	ImBr-PS-POM(Br omide- Functionalized Polyoxometalate)	Styrene oxide (10 mmol), catalyst (20 mg), CO ₂ , CH ₃ CN solvent, 10 h, 500 W Xe lamp, photocatalytic.	99	<i>ACS Sustainable Chem. Eng.</i> 2024, 12 , 16396–16408
8.	Al ₂ O ₃ /CoAl ₂ O ₄	Styrene oxide (5 mmol), TBAI (0.1 mmol, 36.5 mg); 15% Co-Al ₂ O ₃ (10 mg); CO ₂ , temp (27 °C), photocatalytic.	43	<i>Inorg. Chem.</i> 2025, 64 , 1808–1820
9.	Bi-single-atom supported on ZnO nanosheet (Bi/ZnO)	Styrene oxide (0.61 mmol), TBAB (5 mg), DMF (2 mL), 1 bar CO ₂ , catalyst (10 mg), 300 W xenon lamp with a standard AM 1.5 G filter, 12 h., photocatalytic.	81	<i>Sci. China Chem.</i> 2024, 67 , 2292–2299.

10.	Co@BiPy-POP(M-POP)	Styrene oxide(0.5 mL), cocatalyst (160 mg), Photocatalyst (30 mg), CO ₂ 1 atm, blue LED light, photocatalytic.	98	<i>Small</i> 2024, 20 , 2305307
11.	Calix[6]arene-functionalized titanium-oxo clusters	Styreneoxide (4.0 mmol), TBAB (0.30 mmol), CO ₂ (1 atm), catalyst (15 mg), RT, 10 W 430 nm LED, 20 h., photocatalytic.	96	<i>Inorg. Chem. Front.</i> , 2024, 11 , 3755–3764
12.	FeCo@BPDC	Styreneoxide (5 mL), TBAB (0.5 mmol), CO ₂ (1 atm), catalyst, temperature, UV, solvent free, photo-thermal.	25	<i>Catal. Sci. Technol.</i> , 2024, 14 , 3201–3210
13.	Cerium phenylphosphonate (CPP)	Styrene oxide (3 mmol), catalyst (25 mg), PEG 600 (2 mL), TBAB (0.3 mmol), 1 atmCO ₂ , 365 nm light (8 Watt), 12 h., photocatalytic.	95	This work

References

1. J. P. Perdew, K. Burke and M. Ernzerhof, *Phys. Rev. Lett.*, 1996, **77**, 3865.
2. G. Sun, J. Kürti, P. Rajczy, M. Kertesz, J. Hafner and G. Kresse, *J. Mol. Struct. THEOCHEM*, 2003, **624**, 37-45.
3. G. Kresse and J. Furthmüller, *Phys. Rev. B*, 1996, **54**, 11169.
4. G. Kresse and D. Joubert, *Phys. Rev. B*, 1999, **59**, 1758.
5. S. Grimme, J. Antony, S. Ehrlich and H. Krieg, *J. Chem. Phys.*, 2010, **132**.
6. W. Tang, E. Sanville and G. Henkelman, *J. Phys.: Condensed Matter*, 2009, **21**, 084204.
7. K. Momma and F. Izumi, *J. Appl. Crystallography*, 2011, **44**, 1272-1276.
8. V. Wang, N. Xu, J. C. Liu, G. Tang and W.-T. Geng, *arXiv preprint arXiv:1908.08269*, 2019.
9. J. Heyd, G. E. Scuseria and M. Ernzerhof, *J. Chem. Phys.*, 2003, **118**, 8207-8215.